1963

Electrochemical processes in fused salts

Lowell Alvin King
Iowa State University

ELECTROCHEMICAL PROCESSES IN FUSED SALTS

by

Lowell Alvin King

A Dissertation Submitted to the
Graduate Faculty in Partial Fulfillment of
The Requirements for the Degree of
DOCTOR OF PHILOSOPHY

Major Subject: Inorganic Chemistry

APPROVED:

Signature was redacted for privacy.
In Charge of Major Work

Signature was redacted for privacy.
Head of Major Department

Signature was redacted for privacy.
Dean of Graduate College

Iowa State University
Of Science and Technology
Ames, Iowa

1963

TABLE OF CONTENTS

PART I. DIRECT CURRENT MEASUREMENT OF FUSED SALT CONDUCTIVITY

INTRODUCTION AND LITERATURE SURVEY

The high specific conductivity of most fused salt systems complicates the usual alternating current measurement techniques. In order to achieve sufficiently high total resistance in a conductivity cell, it is necessary to resort either to a long current path, or to a small diameter cell. Typically, a glass capillary, filled with fused salt, is used. Glass itself becomes relatively conductive at high temperatures, and may cause significant error in conductivity measurements. Furthermore, any attack of the cell wall by a melt will cause a greater relative cell constant change in a small diameter cell than in a larger diameter cell, and will be reflected in a larger conductivity error in the former case.

Direct current conductivity measurements permit simple cell design, reduce the probability of significant error due to conductance through glass, and allow the use of quite simple electrical circuitry. On the other hand, such a technique suggests at least two possible sources of trouble. First, it must be demonstrated that there is nothing about the mechanism of electrical conductance which would display a frequency dependence. Secondly, conveniently prepared and used reversible electrodes must be available to measure voltage drop in the conductivity cell. Such electrodes are not necessarily easily devised for use in fused salt systems.

The primary purpose of this research is to demonstrate the practicability of using a direct current technique to measure the conductivity of fused salt systems.

A few studies of aqueous solution conductivities have been carried out by a direct current method. These studies involved basically the same experimental approach that was followed in this research; viz., the voltage drop across a known path length of solution was measured by a pair of some sort of reference electrodes as current was passed through the solution. This is the so-called "four-probe" method, where the two reference electrodes and two working electrodes (carrying current into and out of the solution) constitute the four probes. Typically, the reference electrodes were either calomel or Hg_2SO_4 (1,2). Other studies employed reference electrodes of platinum which first were silver plated then chloridized (3,4). Ives and Swaroopa (5) used silver-silver chloride, quinhydrone, and phthalate-stabilized quinhydrone electrodes. Brönsted and Nielsen (6) used the so-called "two-probe" method, whereby the working electrodes and reference electrodes were the same. They used platinized platinum hydrogen electrodes, claiming to achieve high accuracy even though slight polarization occurred.

In 1920, Eastman (7) proposed the idea that direct current conductivities might differ from alternating current values, but found d.c. and 1000-cycle values for the con-

ductivity of 1 N KCl to agree to within 0.02 to 0.03%. At about the same time, Newberry (2) obtained fair agreement with the then accepted a.c. values for three salts, including 1 N KCl. Both Eastman and Newberry obtained significantly low results on H_2SO_4 solutions. More recently, Andrews and Martin (1), Gunning and Gordon (3), and Kell and Gordon (4) have studied extensively the d.c. conductivity of LiCl, NaCl, and KCl solutions. It now appears quite clear that at least for solutions of strong salts (i.e., salts which are highly dissociated and do not hydrolyze) d.c. conductivities are not sensibly different from a.c. conductivities. Accordingly, the cells used in this research were calibrated with aqueous KCl.

It was mentioned above that Eastman (7) and Newberry (2) had found low d.c. conductivities for H_2SO_4. Brönsted and Nielsen (6) investigated a number of solutions of HCl and of H_2SO_4 at different concentrations, but did not independently determine their cell constants. Therefore, their results cannot be said to agree or disagree with a.c. values. It is well known that the ionic conductance of H^+ and of OH^- are abnormally high. It has been suggested that the high conductivity of these ions may arise from some sort of Grotthuss chain mechanism (8). Bissell[1] has shown that d.c. conduc-

---

[1]Bissell, C. L., Ames, Iowa. Unpublished data on direct current conductivity of NaOH solutions. Private communication. 1962.

tivities of 0.7 N, 1.2 N, and 5.0 N NaOH agree with a.c. values. The status of strong acid d.c. conductivity must be considered an open question. Direct current data on HCl are presented in this work.

Poincaré (9) was the first investigator to measure fused salt conductivities by a direct current method. This work was done in 1890. He used the four-probe technique. His data showed considerable scatter and were often in serious disagreement with alternating current values which have been obtained since. So far as the author is aware, no d.c. measurements on fused salt systems have been published since the appearance of Poincaré's work.

Grantham and Yosim (10) have compared alternating current with four-probe and two-probe direct current conductivities in molten Bi-BiI_3 solutions. They used a capillary cell with bare tungsten electrodes in all cases. They found that all three methods gave results agreeing to within 0.1%.

The systems chosen in this research to demonstrate the utility of the direct current technique in fused salts were $LiNO_3$, $NaNO_3$, KNO_3, and binary mixtures of these salts. Alternating current conductivities of these systems are known (11,12,13,14,15,16,17,18,19,20,21,22) and will be compared below with the findings of this research.

EXPERIMENTAL

Materials and Equipment

Chemicals

"Baker analyzed" reagent $AgNO_3$, Fisher certified reagent KCl, and Baker and Adamson reagent HCl were used without further purification. "Baker analyzed" reagent $LiNO_3$, $NaNO_3$, and KNO_3 were treated in the following manner: The salts, or salt mixtures, were weighed, then melted in a 1-liter round-bottom flask and allowed to stand molten for 12 to 24 hours. To insure good mixing, the binary nitrate melts were thoroughly stirred for at least an hour while molten. The $LiNO_3$ was dried at 135° for at least 24 hours before it was melted.

Each melt was filtered through a medium or fine porosity 30-mm sealing tube and allowed to cool in small porcelain crucibles. The resulting salt pellets were stored in a $Mg(ClO_4)_2$-charged desiccator before use.

Conductivity water for HCl and KCl solutions was prepared by passing tap distilled water through a Barnstead "Bantam" demineralizer column (Barnstead Still and Sterilizer Co., Boston, Mass.). From time to time the conductivity of the demineralized water was measured to insure that it was, indeed, of conductivity quality.

Furnace and temperature control

A 12-inch Marshall tube furnace (Marshall Products Co., Columbus, Ohio), mounted vertically, was used to heat the conductivity cells. This furnace was provided with 8 taps on the heater winding, across which appropriate shunts could be placed to maintain any desired temperature gradient along the axis of the furnace cavity. Shunts of various resistances, empirically determined, were placed across the taps such that at a furnace temperature near 280°, the temperature gradient across the voltage drop region of the conductivity cell was 0.9°. This gradient increased to 1.6° at a furnace temperature near 415°.

A Pyrex-sheathed chromel-alumel thermocouple, immersed in the central tube of the conductivity cell, led to a Bristol "Series 536 Free-Vane Electronic Indicating Controller" (The Bristol Co., Waterbury, Conn.). The controller turned on and off electric power to the furnace, as supplied by a 110-volt Powerstat. Once thermal equilibrium was reached within the furnace, a given cell temperature could be maintained to within less than a degree.

Conductivity cells

Two Pyrex conductivity cells were used. These cells were quite similar in design, differing slightly in dimensions. Figure 1 shows one of these cells. Direct current was passed through the main channel of the U-tube and the

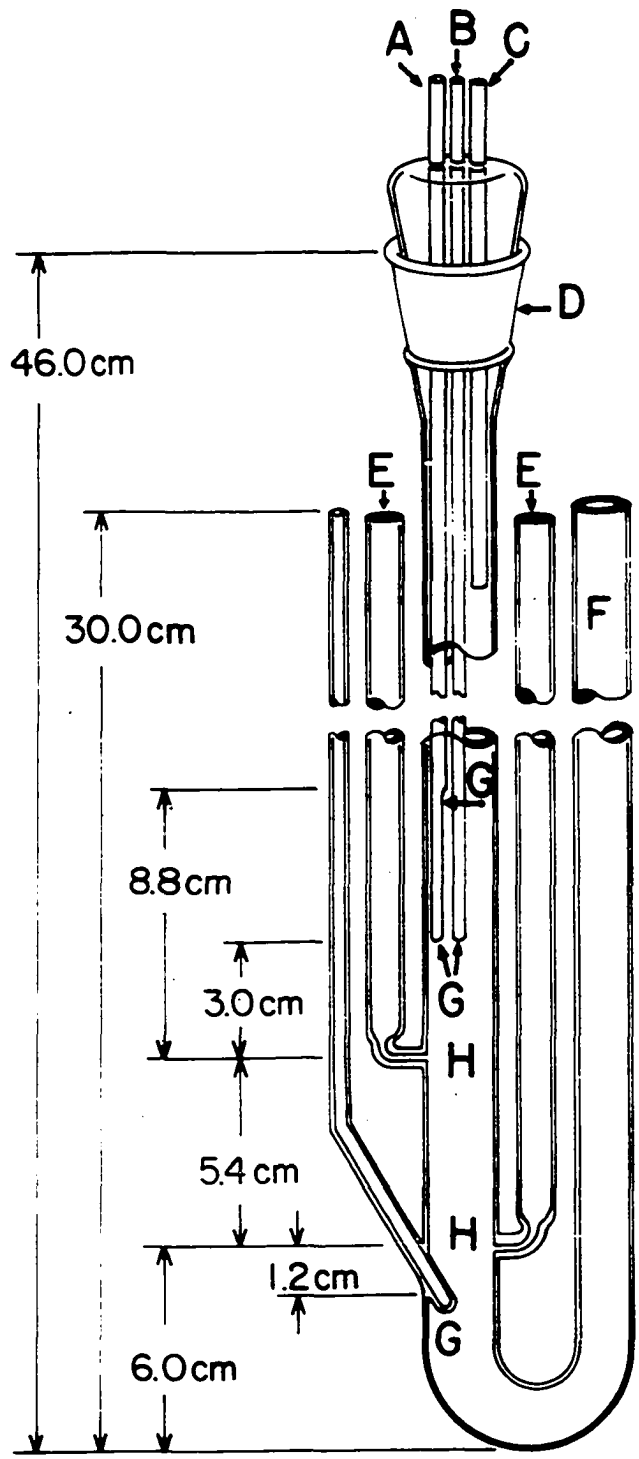

A- 5mm ID DUAL THERMOCOUPLE WELL

B- 3mm ID THERMO-COUPLE WELL

C- 5mm ID ELEC-TRODE ACCESS PORT

D- 29/42 STANDARD TAPER ON 17mm ID CENTRAL TUBE

E- 8mm ID SIDE-ARMS

F- 13mm ID TUBE

G- THERMOCOUPLE LOCATIONS

H- 1mm DIA. HOLES LEADING TO SIDE-ARMS

Figure 1. Conductivity cell

voltage drop between points H (see Figure 1) was measured by reference electrodes in the side-arms. Provision was made in each cell for the immersion of four thermocouples in the melt. One thermocouple led to the controller, and the other three were used to determine salt temperature in the voltage drop region, as will be discussed below.

Cell constants were determined from the direct current conductivity of 1-demal KCl, prepared according to the specifications of Jones and Bradshaw (23). Cell constants were corrected for the thermal expansion of Pyrex by the equation

$$k_t = \frac{k_{25}}{1 + \alpha t}$$

where

k_{25} = cell constant at 25°

α = coefficient of linear expansion of Pyrex

= 3.6×10^{-6} deg^{-1} (24)

t = °C-25

k_t = cell constant at temperature t.

Silver-silver nitrate electrodes were used in the side-arms to register the potential developed across the voltage drop region. These electrodes consisted of small Pyrex tubes, open at the top, and terminating in thin-walled bubbles to provide electrical contact to the melt in the conductivity cell. The electrodes were partially filled with a solution 10% by weight $AgNO_3$ in equimolar $NaNO_3$-KNO_3.

Silver wires dipped into the silver nitrate solutions and extended out the tops of the tubes. Similar electrodes have been described by Inman (25).

The silver-silver nitrate electrodes showed no measurable polarization to be caused by the minute current necessarily passed through them in the process of adjusting the potentiometer used to measure voltage drop.

Beckman model 39270 calomel electrodes were used in the side arms for all experiments on aqueous solution conductivity.

Platinum wire helices were used to supply direct current to the conductivity cell.

Temperature measurement

Three chromel-alumel thermocouples were used to determine the temperature of the voltage drop region of the conductivity cell (see Figure 1). One thermocouple was located in the well below the side arms, and two others were located at points G in tube A. The average temperature in the voltage drop region was found to be satisfactorily calculated from the equation

$$\bar{t} = t_m - \frac{1}{3}(t_m - t_b)$$

where

$\bar{t}$ = average temperature in the voltage drop region

t_m = temperature indicated by the middle thermocouple

t_b = temperature indicated by the bottom thermocouple.

The uppermost thermocouple served to insure a minimum

liquid level in the conductivity cell; if the thermocouple were not immersed, it would indicate an abnormally low temperature.

The thermocouple wires were encased in small alundum tubes, and the whole assembly protected from contact with molten salt by Pyrex sheathing. An ice bath cold junction was used. Thermocouple voltage was measured by a Fisher "Type S" potentiometer and a Leeds and Northrup "Type 2420 A" galvanometer. The three thermocouples were jointly calibrated in freezing $NaNO_3$. They indicated temperatures too low by 1.0, 1.0, and 1.75 degrees. The data presented in this study are corrected for thermocouple error.

Water bath

When used to measure aqueous solution conductivities, the conductivity cells were maintained at $25.00 \pm 0.02°$ in a large, stirred water bath. The bath was cooled by cold tap water circulating through coiled tubing and was heated by a Cutler Hammer 500-watt heater. Heater operation was controlled by a Precision Scientific Co. "Micro-Set Differential Range Thermoregulator" and electronic relay. Temperature accuracy was assured by periodic checking against a calibrated Emerson calorimetric thermometer.

Electrical circuits

The electrical circuits employed in this research are shown in Figure 2. Direct current was drawn either from a

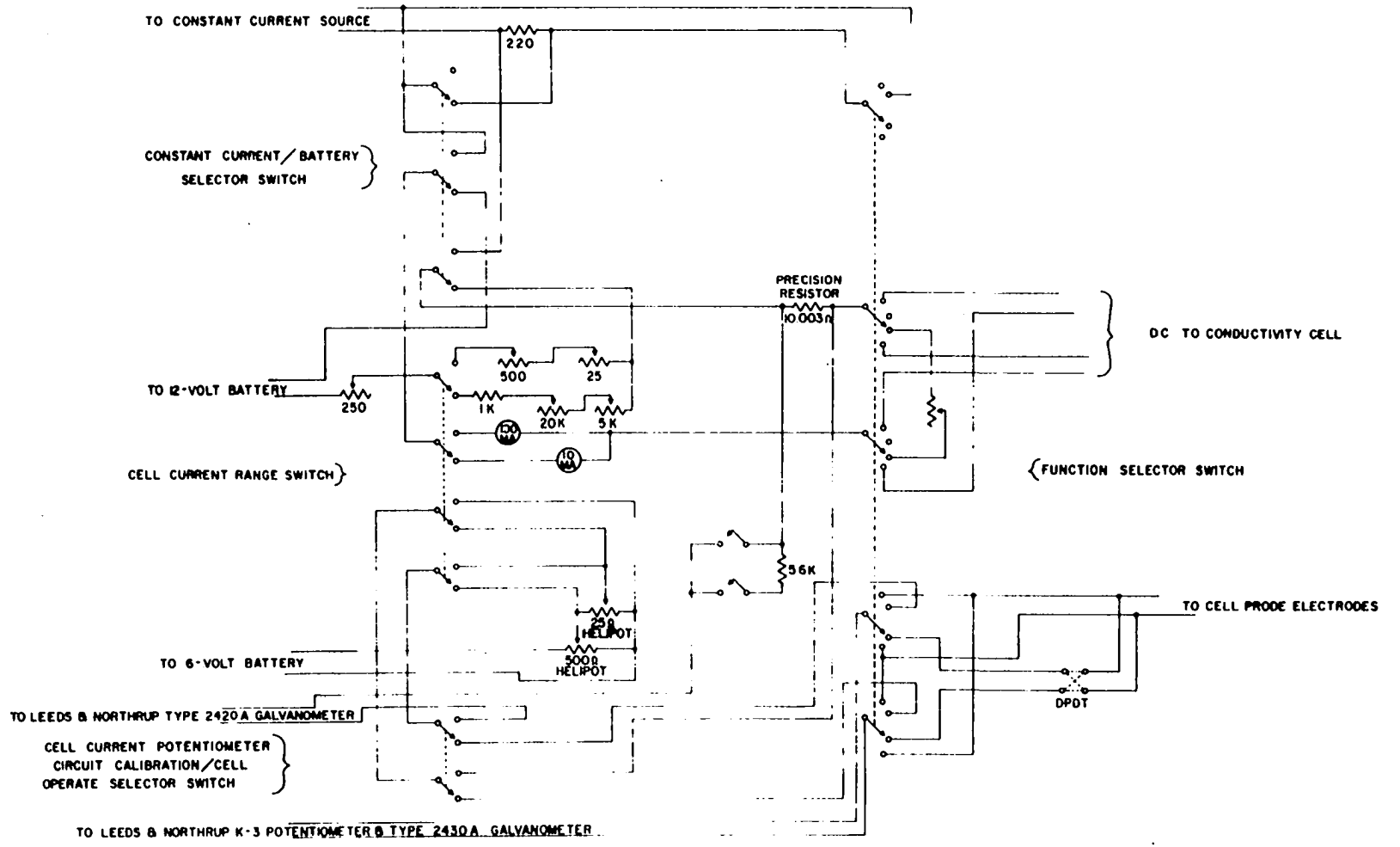

Figure 2. Electrical circuits

12-volt storage battery bank or from a constant current supply.[1] The constant current supply was available only for the later experiments. It greatly facilitated the convenience and rapidity of data collection. The current was led through a Gray Instrument Co. 10-ohm precision resistor to the "function selector switch". The 10-ohm resistor was calibrated by means of a Leeds and Northrup Mueller Temperature Bridge together with a Leeds and Northrup Electronic D-C Null Detector; its resistance was 10.003 ohms. When the 12-volt battery was used as the current source, a series of variable resistors was included in the current path. These resistors provided rapid manual control of current strength. The constant current source had its own current control adjustments.

The "function selector switch" controlled access of current to the conductivity cells. When the switch was in either extreme position, current passed through the molten salt. The two positions were of opposite polarity. It will be noted that two pairs of current leads go to the conductivity cell. Each pair terminated in a pair of concentric platinum helices, which were the actual working electrodes. Because of electrode polarization the effective total cell resistance would change markedly and rapidly as current

[1]The constant current supply was designed by R. N. Kust, Ames, Iowa.

polarity was reversed if single electrodes were used. This resistance change, in turn, made current control extremely difficult when the 12-volt battery was the current source. For this reason, electrode pairs were used, each member of each pair always being used to conduct only in one direction. The constant current supply automatically and efficiently compensated for changes in effective total cell resistance, and made the use of electrode pairs unnecessary. Accordingly, the two leads of each pair of leads were joined, and single electrodes used in the later experiments.

As may be seen from Figure 2, the 500-ohm and 25-ohm Beckman Helipots constitute a potentiometric circuit for measuring voltage drop across the 10-ohm precision resistor. In practice, current was adjusted such that for a given Helipot setting, depression of the tap switches caused no deflection in the Leeds and Northrup type 2420-A galvanometer. A given Helipot setting provided for two current values, selected by the "cell current range switch". The Helipots could be set for any desired cell current by calibration with the Leeds and Northrup type K-3 potentiometer. Such calibration was accomplished by appropriately positioning the "function selector switch" and the "cell current potentiometer circuit calibration/cell operate selector switch". When the Leeds and Northrup type 2430-A galvanometer showed no deflection, the number of millivolts to which the K-3 potentiometer

was set divided by 10.003 was numerically equal to the number of milliamperes of cell current for which that given Helipot setting was adjusted.

The two lower gangs of the "function selector switch" connect the side-arm electrodes to the K-3 potentiometer. Electrode polarity was automatically changed as cell current polarity was changed. Provision was also made for measuring the potential difference between the side-arm electrodes when no current was flowing through the cell. Such a provision made possible a convenient check on polarization and on the inevitable deterioration of the side-arm electrodes.

Method of Operation

Determination of cell constants

The conductivity cells were well rinsed with 1-demal KCl, filled with that solution, and allowed to thermally equilibrate with the 25° water bath. The working electrodes and calomel reference electrodes were inserted and current passed through the cell in one direction. The potential difference between the reference electrodes was recorded. Then the cell current was reversed and the new potential difference was recorded. The reference electrode potential difference at zero-current was measured before and after each of the above operations. The electrodes were then removed and washed and the cell sealed for a period of several minutes to

several hours, whereupon the measurement cycle was repeated at some different cell current. After a number of such cycles, the cell was emptied, refilled, and the whole operation repeated.

At any given current value, the potential differences measured were averaged for forward and reverse current. If this average did not agree with the average of the potential differences as corrected for zero-current voltage, the data were discarded.

All of the individual cell constant determinations carried out in the manner just described were averaged for each cell. It is believed that the resulting cell constants were accurate to within 0.01%.

Cell constants were redetermined after most of the fused salt experiments were completed, and were found to be unchanged within the accuracy of the fused salt conductivity measurements.

Measurement of hydrochloric acid conductivities

Hydrochloric acid conductivity measurements were made in the same manner as with 1-demal KCl.

The HCl solutions were standardized gravimetrically by precipitation of AgCl with $AgNO_3$. The analysis was carried out in the manner recommended by Diehl and Smith (26).

Measurement of fused salt conductivities

The conductivity cell was preheated to some temperature above the melting point of the salt whose conductivity was to

be determined and the salt or salt mixture added. The platinum working electrodes and the silver-silver nitrate reference electrodes were then put into place. Once thermal equilibrium was reached (as indicated by the absence of temperature fluctuations at the thermocouple locations), conductivity measurements were commenced. The sequence of steps was as follows:

1. Measure temperature in voltage drop region.
2. Measure potential difference between the reference electrodes at zero cell current.
3. Measure potential difference between the reference electrodes as current is passed through the cell.
4. Repeat step 2.
5. Repeat step 3 at the same current value, with reversed polarity.
6. Repeat step 2.
7. Repeat step 1.
8. Repeat steps 2 through 7 at some different cell current value.

The entire sequence of steps was repeated at each new furnace temperature setting. Normally, the first conductivity measurements were made just above the melting point of the salt being investigated, and furnace temperature was increased in steps until either the electrodes failed or the salt began to decompose. In some cases, however, furnace

temperature was changed in random order, or was reset to some previously used temperature. Observed conductivities did not appear to depend on the order of temperature settings.

The cell current potentiometer circuit (Helipots) was calibrated at sufficiently frequent intervals to insure continually accurate cell current determination.

Calculations

Ideally, specific conductivity may be calculated from the equation

$$\kappa = \frac{\ell I}{\pi r^2 E}$$

where

κ = specific conductivity, ohm^{-1} cm^{-1}

ℓ = distance between side-arm holes, cm

I = cell current, amperes

r = radius of U-tube in voltage drop region, cm

E = voltage drop, volts.

In practice, it is not convenient to determine ℓ and r as accurately as is required, nor to insure uniformity of r. For this reason, specific conductivity is usually calculated from the equation

$$\kappa = \frac{kI}{E}$$

where k is the cell constant, and includes implicitly the real values of ℓ and r and any variations of r.

Equivalent conductivity of aqueous solutions was

calculated from the equation

$$\Lambda = \frac{1000\kappa}{N}$$

where

Λ = equivalent conductivity, ohm^{-1} cm^2 $equiv.^{-1}$

N = normality, equiv. $liter^{-1}$.

Equivalent conductivity of fused salt systems was calculated from the equation

$$\Lambda = \frac{\kappa}{\rho} \sum_i X_i E_i$$

where

ρ = density, gm cm^{-3}

X_i = mole fraction of salt i

E_i = equivalent weight of salt i.

RESULTS AND DISCUSSION

Conductivity Cell Performance

As Gunning and Gordon have pointed out (3), it is essential to consider two important problems in planning an experiment involving the four-probe technique. It is necessary first of all that the reference electrodes be reversible. Non-reversibility or polarization of electrodes in the conventional alternating current experiments is detectable as a frequency dependence and as a current strength dependence of the apparent solution conductivity. If non-reversibility or polarization is a problem, suitable corrections can be made and meaningful conductivities calculated.

Non-reversible or polarized electrodes become more difficult to treat in a d.c. technique. For one thing, frequency is always zero. Any frequency effect will be unobservable. It is also true that any non-reversibility of the reference electrodes will not always be apparent when one is in the process of measuring voltage drop. Severe cases of polarization may be reflected in an unstable measured voltage drop, and may be alleviated by drawing only extremely minute currents from the reference electrodes (for example, while searching for the null-point with a potentiometric circuit).

The calomel electrodes employed in this work (aqueous solutions) behaved very satisfactorily and gave no reason to

suspect error to be introduced through polarization or lack of reversibility. When on occasion relatively large voltages were accidently applied across these electrodes, rapid and complete recovery of their "open circuit" voltages was observed. So, too, did the silver-silver nitrate electrodes (fused salt solutions) behave well. As was mentioned earlier, every conductivity determination was made with both forward and reverse cell currents. Each measurement was also accompanied by notation of the potential difference between the reference electrodes both before and after the actual run. These two operations constituted a continual monitoring of and correction for residual reference electrode voltage asymmetry, and also warned of any development of electrode deterioration.

The most serious shortcomings of the silver electrodes were their limited useful temperature range and their sensitivity to melt composition. At temperatures below about 300° the Pyrex bubbles became quite non-conductive and it was difficult to determine null-points accurately. As might be expected, this sluggish response was most pronounced at higher mole fractions of KNO_3, due, presumably, to the large cationic radius of potassium. At temperatures in excess of 400°, the silver electrodes did not work well in melts of high $LiNO_3$ concentrations. The reasons are not clear. Once an electrode was exposed to temperatures above 400° in lithium-rich melts

it either failed completely or recovered its reversibility upon cooling.

One could presumably circumvent the lack of electrode sensitivity at cooler temperatures in either of two ways. One could use some ultra-high impedance instrument (such as an electrometer) rather than a galvanometer as the null indicator. Alternatively, one might go to an electrode such as that of Duke and Garfinkel (27), who provided electrical contact between the silver solution and the outside melt by means of a glass frit. No suitable high impedance instrument was available when this work was performed. Glass frits were tried in preliminary experiments but their use was discontinued in view of the inconvenience of coping with their tendency to leak through the frit.

The second problem pointed out by Gunning and Gordon (3) is concerned with electrode geometry. Ideally, a reference electrode should be vanishingly small in the dimension parallel to the flow of cell current. To the degree that this requirement is not met, voltage drop occurs across the surface of the electrode itself, and the conductivity of the solution being studied will appear to depend upon current strength.

The glass blower who made the conductivity cells was instructed to make the U-tube holes which led to the side-arms as small as was practicable. He was also instructed to be

sure that no significant outward bulge in the U-tube walls appeared at the hole locations. The principal reason these precautions were taken was to minimize the effective reference electrode relative size in the direction parallel to current flow. (It is reasonable to assume that the potential difference between the hole sites would be equal to that seen in the side-arms at the actual electrode locations. At any rate, any voltage developed within the side-arms would cancel as the cell current was reversed). As evidence of successful elimination of cell current effects, specific conductivities did not change within experimental error as the current was changed 40-fold in the fused salt experiments and 16-fold in the aqueous solution experiments.

It should be mentioned that Ives and Swaroopa (5) have circumvented the problem of reference electrode geometry in another way. Their cell was designed in such a way that reference electrode access to the voltage drop region occurred in regions of essentially zero potential gradient. Their cell, however, was necessarily of rather complex design, and would not be well suited for fused salt work in instances where such severe attack upon the cell occurs that a new cell would be required for each salt composition studied.

The two cell constants were 109% and 95% of the values which were calculable from cell geometry. Considering the difficulty of precisely measuring the inside diameter of the

U-tubes in the voltage drop region, such close agreement of cell constants to theoretical values is powerful evidence that the method of direct current conductivities is valid.

Aqueous Solution Conductivities

The d.c. specific conductivities of the hydrochloric acid solutions investigated in this research are shown in Table 1. Table 2 compares the present equivalent conductivities with the most recently published and most carefully measured alternating current values. The agreement was not as good as one might have hoped, especially at the lower concentrations. On the other hand, the results are at least as good as those obtained with H_2SO_4 (2,7) and suggest that nothing about the chain process of hydrogen ion migration leads to a large frequency dependence of conductivity.

It is worthwhile considering the possibility that at the HCl concentrations used in this work hydrogen ion-chloride ion pair formation might impede functioning of the hydrogen ion chain (28). If this were so, and if there were a frequency effect on the chain, then the fact that the a.c.-d.c. discrepancy found in this research was greatest in the most dilute solution is explained.

Fused Salt Conductivities

The results obtained in the present work for direct current specific conductivities of alkali metal nitrates are

Table 1. Specific conductivity of hydrochloric acid solutions at 25 °C

HCl concentration, moles/l	κ, ohm^{-1} cm^{-1}	average κ, ohm^{-1} cm^{-1}
0.4434	0.16209	
	0.16210	
	0.16199	0.1620_6
1.043	0.34437	
	0.34486	
	0.34469	
	0.34461	
	0.34470	
	0.34482	
	0.34498	0.3447_2
2.083_5	0.58103	
	0.58082	
	0.58097	
	0.58074	
	0.58080	
	0.58080	0.5808_6

Table 2. Equivalent conductivity of hydrochloric acid solutions at 25 °C

HCl conc., moles/l	Λ, $ohm^{-1}cm^2$ equiv.$^{-1}$ This work	Owen & Sweeton[a]	difference, %[b]	Stokes[c]	difference, %[b]
0.4434	365.5	364.1	+0.38	364.41	+.30
1.043	330.5	330.1	+0.12		
2.083_5	277.8	277.6	+0.072		

[a]Graphical interpolation from a large scale plot of Λ vs. $(conc.)^{\frac{1}{2}}$ as reported by Owen and Sweeton (28).

[b]Calculated by $\left(\frac{\text{this work-lit. value}}{\text{this work}}\right)$ 100.

[c]Calculated from the interpolation function of Stokes (29).

presented in Table 3. The data were sufficiently precise that smooth curves could easily be drawn through the values when plotted. Accordingly, the empirical equations of Table 4, relating conductivity to temperature, were obtained by the method of selected points (30). These equations represent the data to within experimental error.

The present results are compared to values obtained by other workers (all of whom used alternating current techniques) in Figure 3. Only the curves for the pure salts are shown. It is evident that the d.c. results are in excellent agreement with the a.c. values. Similar agreement was noted for those binary melts for which literature values were available. It is interesting to observe that the $LiNO_3$ data, unlike all of the others, form a curve which is slightly concave upward. Such behavior is not generally observed, as Popovskaya and Protsenko (20) have shown for a variety of pure nitrates of monovalent cations and for some of their binary mixtures. Lithium nitrate was the last salt investigated during this research, for it was expected that some attack on the cell would take place. Furthermore, for this reason, data were taken in order of ascending temperature. Such an attack did occur to a slight extent, as evidenced by the Pyrex becoming frosted and cracking upon cooling. If the attack were accompanied by a slight increase in U-tube radius, then the voltage drop would be less than expected,

Table 3. Experimental values of specific conductivity of $LiNO_3$, $NaNO_3$, KNO_3, and their binary mixtures

Melt composition, mole %	Temperature, °C	κ, ohm^{-1} cm^{-1}	Melt composition, mole %	Temperature, °C	κ, ohm^{-1} cm^{-1}
100 $LiNO_3$	284.2	0.9676	50.0_4 $LiNO_3$	283.8	0.9097
	284.2	0.9696	49.9_6 $NaNO_3$	283.8	0.9175
	321.8	1.1756		303.6	1.0171
	321.8	1.1786		303.6	1.0185
	359.0	1.3880		331.5	1.1472
	359.0	1.3884		331.5	1.1560
				355.1	1.2642
100 $NaNO_3$	330.5	1.089		355.1	1.2645
	330.5	1.090		394.2	1.4443
	349.0	1.168		394.2	1.4465
	349.0	1.175			
	398.6	1.382	74.6_0 $LiNO_3$	285.8	0.9563
	398.6	1.383	25.3_0 $NaNO_3$	286.2	0.9576
	444.5	1.558		319.5	1.130
	444.5	1.562		319.5	1.133
				358.5	1.330
100 KNO_3	354.0	0.6785		359.0	1.329
	354.0	0.6789		397.8	1.53
	374.8	0.7442			
	374.8	0.7470	23.3_1 $LiNO_3$	278.5	0.5139
	398.2	0.8181	76.6_9 KNO_3	279.6	0.5236
	398.6	0.8190		302.6	0.5974
	422.2	0.8882		302.6	0.5977
	422.2	0.8894		325.8	0.6761
				326.0	0.6772
25.0_5 $LiNO_3$	278.5	0.8651		350.2	0.7616
74.9_5 $NaNO_3$	278.5	0.8660		350.6	0.7626
	300.8	0.9763		374.2	0.8398
	300.8	0.9777		374.2	0.8419
	327.2	1.096		396.8	0.9172
	327.2	1.099		397.2	0.9180
	348.8	1.199		421.0	0.9951
	349.2	1.203		421.2	0.9949
	375.2	1.319			
	375.3	1.320	50.1_2 $LiNO_3$	285.5	0.6445
	398.6	1.422	49.8_8 KNO_3	286.9	0.6489
	398.8	1.422		312.0	0.7419
	421.8	1.516		312.7	0.7440
	421.8	1.516		345.0	0.8685

Table 3. (Continued)

Melt composition, mole %	Temperature, °C	κ, ohm^{-1} cm^{-1}	Melt composition, mole %	Temperature, °C	κ, ohm^{-1} cm^{-1}
	345.1	0.8688	50.31 $NaNO_3$	280.8	0.5989
	381.5	1.0048	49.69 KNO_3	282.2	0.6014
	381.5	1.0048		325.5	0.7730
	427.2	1.18		326.2	0.7746
				375.8	0.9555
74.8_0 $LiNO_3$	290.2	0.8025		375.8	0.9556
25.2_0 KNO_3	290.2	0.8034		398.8	1.038
	330.2	0.9838		399.0	1.039
	330.2	0.9866		422.2	1.117
	370.2	1.155		423.2	1.118
	370.8	1.154			
			75.09 $NaNO_3$	301.8	0.7923
24.85 $NaNO_3$	280.0	0.5125	24.91 KNO_3	302.1	0.7957
75.15 KNO_3	280.0	0.5128		302.1	0.7971
	302.6	0.5929		302.8	0.7957
	302.6	0.5930		348.8	0.9909
	326.0	0.6741		348.8	0.9977
	326.2	0.6749		398.8	1.187
	352.0	0.7624		398.8	1.190
	352.2	0.7620			
	376.8	0.8429			
	377.0	0.8435			
	399.0	0.9159			
	399.0	0.9165			
	420.8	0.9836			
	421.0	0.9841			

Table 4. Specific conductivity equations for $LiNO_3$, $NaNO_3$, KNO_3, and their binary melts

melt composition, mole %	$\kappa = a + bt + ct^2$ a	b x 10^3	c x 10^6
100 $LiNO_3$	-0.4424	4.4524	+1.8027
100 $NaNO_3$	-0.8007	6.9089	-3.5949
100 KNO_3	-0.8241	5.2218	-2.7583
25.0_5 $LiNO_3$ 74.9_5 $NaNO_3$	-0.7763	6.7915	-3.2169
50.0_4 $LiNO_3$ 49.9_6 $NaNO_3$	-0.6253	5.9456	-1.7573
74.6_0 $LiNO_3$ 25.3_0 $NaNO_3$	-0.7441	6.5804	-2.2173
23.3_1 $LiNO_3$ 76.6_9 KNO_3	-0.5769	4.2578	-1.2446
50.1_2 $LiNO_3$ 49.8_8 KNO_3	-0.4578	3.9418	-0.2828
74.8_0 $LiNO_3$ 25.2_0 KNO_3	-0.8902	6.9590	-3.8750
24.85 $NaNO_3$ 75.15 KNO_3	-0.6391	4.6240	-1.8254
50.31 $NaNO_3$ 49.69 KNO_3	-0.7358	5.4550	-2.5391
75.09 $NaNO_3$ 24.91 KNO_3	-0.9017	6.8016	-3.9159

Figure 3. Specific conductivities of $LiNO_3$, $NaNO_3$, and KNO_3

-o- this work
● Jaeger and Kapma (15)
△ Doucet and Bizouard, calculated from their equation (12)
▽ Doucet and Bizouard (13)
▲ Protsenko and Popovskaya (21)
▼ Murgulescu and Zuca (18)
□ Goodwin and Mailey (14)
■ Polyakov (19)
\+ Kröger and Weisgerber (16)
x Sandonnini (22)

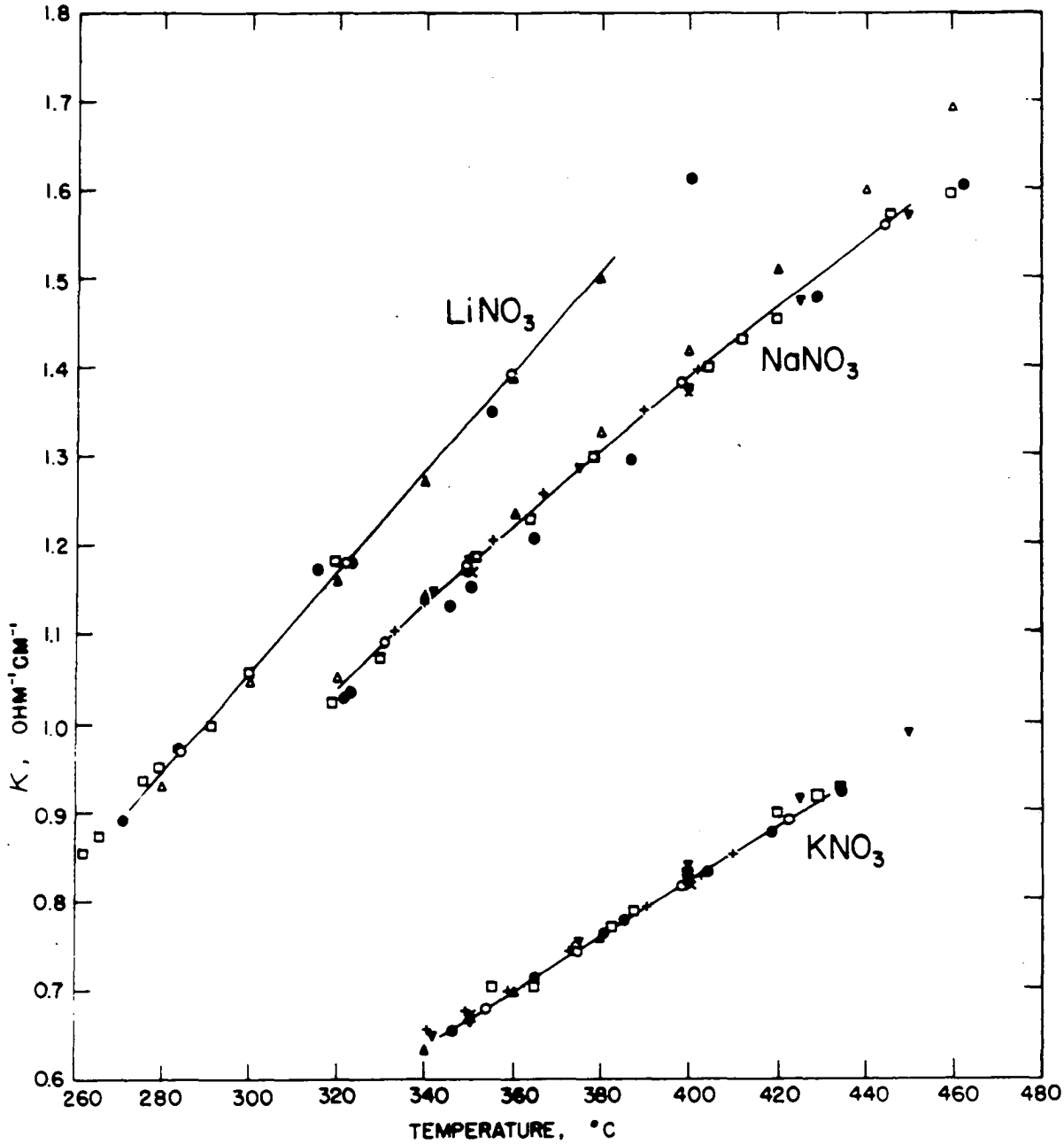
LiNO3
NaNO3
KNO3
K, OHM-1CM-1
TEMPERATURE, °C
1.8
1.7
1.6
1.5
1.4
1.3
1.2
1.1
1.0
0.9
0.8
0.7
0.6
260
280
300
320
340
360
380
400
420
440
460
480

and the apparent conductivity correspondingly high. The cracks precluded a redetermination of the cell constant after the run.

Typical specific conductivity isotherms (350°) for each pair of nitrates are shown in Figure 4. Other isotherms, of course, may be calculated from the equations of Table 4. Of more fundamental interest are equivalent conductivity isotherms, some of which are shown in Figure 5. As has been shown, salt density (or, what amounts to the same thing, equivalent volume) enters into the calculation of equivalent conductivity. It became somewhat of a problem to select density data to use in these calculations. The literature is replete with densities of pure $LiNO_3$ (15,18,31), $NaNO_3$ (11,13,15,18,22,32), and KNO_3 (11,13,15,18,19,22,31,32). More difficult to find are binary melt densities. Sandonnini (22) has investigated lithium-sodium melts and Smith and Petersen (31) have studied lithium-potassium melts. Only in Murgulescu's laboratory have all three mixtures been investigated. In all of these data there is only fair agreement among the various workers. For the sake of internal consistancy, the densities of Murgulescu and Volanschi (32) and of Murgulescu and Zuca (18) were used here.

Of particular interest are the strong deviations of equivalent conductivity from additivity (dashed lines in Figure 5). The deviation is most pronounced for the $LiNO_3$-

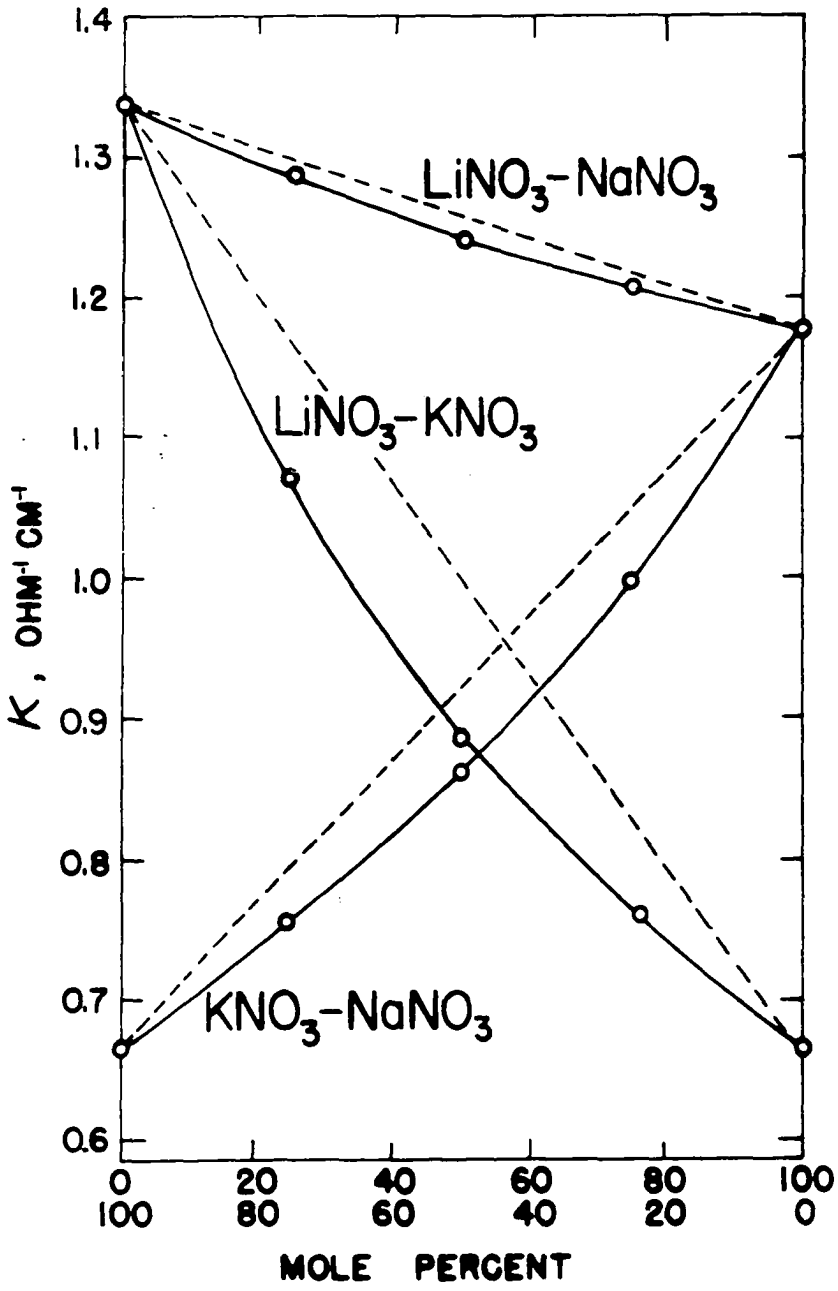

Figure 4. Specific conductivities of binary melts at 350 °C

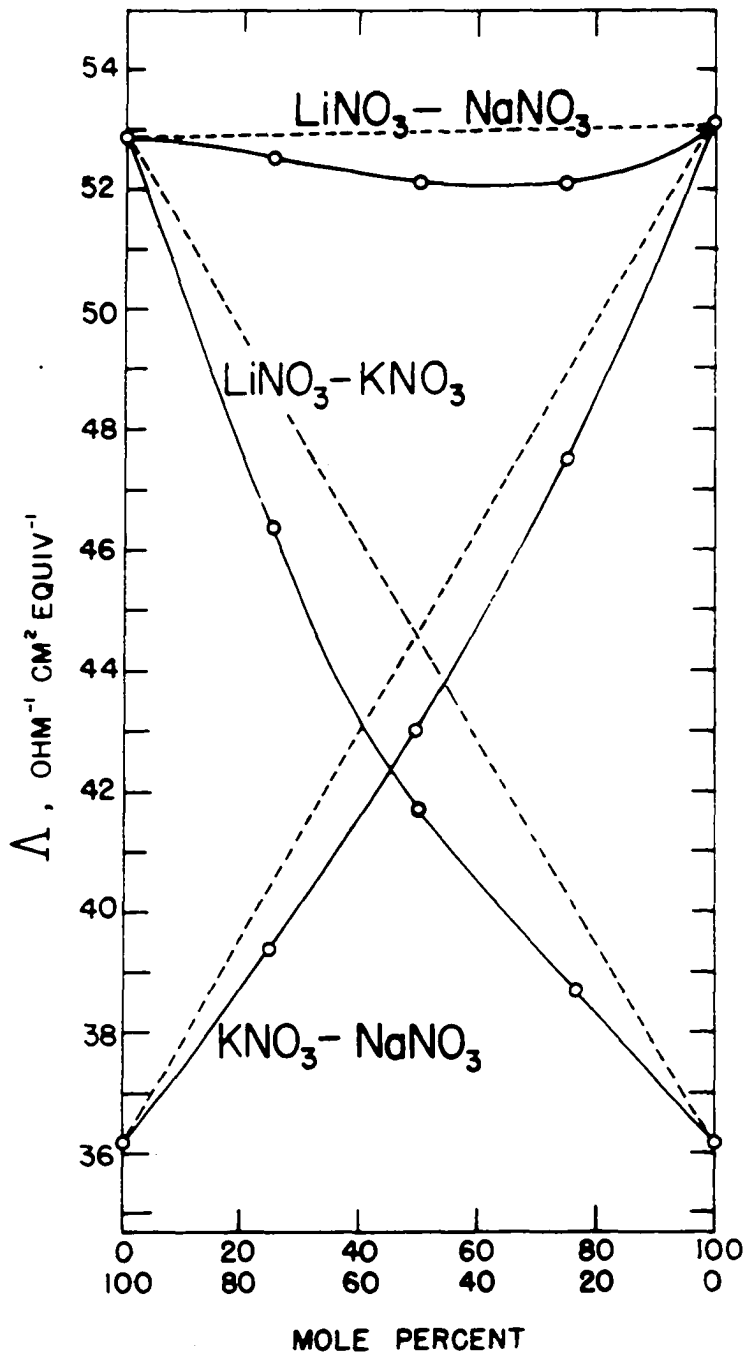

Figure 5. Equivalent conductivities of binary melts at 350 °C

KNO_3 isotherm, where the cationic radius difference is greatest. In the case of $LiNO_3$-$NaNO_3$ melts, all mixtures actually are less conductive than either pure salt. It is highly unusual, but not unique, to observe a minimum in an equivalent conductance isotherm of a melt whose constituents are not readily suspected of any tendency to form complex species. Such behavior has been noted previously for LiCl-KCl[1] (33,34), KCl-KI (34), and possibly NaCl-KCl (34).

It is interesting to inquire into the reasons for the appearance of minima in cases such as those cited and the present work. Unfortunately, no generally accepted explanation is available. Van Artsdalen and Yaffe (34), in discussing their observations of the LiCl-KCl system, propose that short range order in KCl is altered by the presence of low concentrations of small lithium ions such that the chloride lattice becomes shrunken slightly. This in turn would presumably impede the migration of potassium ions, which carry most of the current, leading to a decrease in conductance. Alternatively, they suggest the possibility that potassium would find it more difficult to migrate into lithium cation sites than into potassium sites, the former sites becoming more prevalent as LiCl concentration increases. In either case, the higher mobility of lithium ions would

---

[1]Bissell, C. L., Ames, Iowa. Unpublished data on direct current conductivity of LiCl-KCl melts. Private communication. 1963.

eventually prevail as they become more numerous. It is not clear that either of these suggestions would be wholly satisfactory to explain the present results observed for the $LiNO_3$-$NaNO_3$ system, where analogous behavior occurs on both ends of the isotherm.

An unusual observation by Duke and Victor (35) may be important to any explanation of minima in isotherms of melts similar to those being considered here. For the $LiNO_3$-KNO_3 system, they found that within experimental error each of the cations displayed the same transport number as the other at all concentrations studied, even though the transport numbers were quite different in the two pure salts. They interpreted their results as implying some poly order process being responsible for current conduction, suggesting either motion of groups of ions, or migration of charged holes over relatively large distances in single jumps. Recently, Laity and Moynihan (36) re-examined published data for several other systems and confirmed the approximate equality of cation mobilities.

It is interesting to speculate upon the consequences of assuming the mechanism of Duke and Victor. Suppose one were to consider cationic conduction as consisting of jumps of cation chains. (This is equivalent to considering jumps of charged holes in the opposite direction.) As one added small amounts of one salt to another pure salt, the foreign cations

would become randomly spaced along these chains. It would seem reasonable to assume that if the foreign ions shortened the average chain length, conductivity would decrease. It also seems somewhat reasonable that if chain length were not changed, then the chain non-uniformity might result in an increased activation energy for the jumping process, thereby decreasing conductivity.

Unfortunately, neither a satisfactory theory of fused salts nor sufficient experimental data are available at present; it is not yet possible to explain fully the observed equivalent conductance isotherms in alkali nitrates or similar systems.

Alternate Procedure for Conductivity Measurement

Some preliminary studies were made on a conductivity cell which employed platinum reference electrodes. Short lengths of fine platinum wire were led through the walls of 20 mm ID Pyrex tube. The tube was sealed within another tube to form an air jacket, and the whole assembly partly immersed in the solutions under study. Platinum working electrodes were placed outside the outer tube and inside the inner tube (above the reference electrode). An attempt was made to calculate conductivity from the measured voltage drop across the reference electrodes. In order to minimize electrode polarization, a vacuum tube voltmeter (impedance

of about 10^8 ohms) was employed as a null detector in the potentiometric circuit.

Not surprisingly, the apparent voltage drop varied with time. It was also observed that when current was switched off, a residual voltage of opposite polarity but of approximately the same magnitude appeared across the reference electrodes. A tap switch was devised which permitted conductivity measurements to be made either as current was switched on or switched off. In the former instance, cell current was off, the probes shorted out, and the potentiometer circuit open with the tap switch in rest position. As the switch was depressed the following steps occurred in sequence:

1. Probe short removed
2. Cell current on
3. Potentiometer circuit closed.

The sequence was reversed as the switch was released. The whole cycle was repeated at various potentiometer settings until the null point was found.

In the second method, the cell current was on, the probes shorted out, and the potentiometer circuit open when the tap switch was in rest position. As the switch was depressed the following steps occurred in sequence:

1. Probe short removed
2. Cell current off

3. Potentiometric circuit closed.

As before, the sequence was reversed as the tap switch was released, and the whole cycle repeated until null point was achieved.

Both methods were used to measure the specific conductivities of saturated aqueous NaCl (24°) and of $NaNO_3$-KNO_3 eutectic (238°). Conductivities calculated by each method agreed to within 15% of published values, both for the aqueous system and for the nitrate melt.

It appeared that simple reference electrodes such as those just described might be made to work as well as silver-silver nitrate electrodes, providing polarization could be eliminated. One approach which could be tried would be the use of an ultra-high impedance null point detector in place of a vacuum tube voltmeter. No further experimental work was done on this technique.

SUMMARY

The practicability of direct current specific conductivity determinations of fused salt systems has been demonstrated. A conductivity cell design has been achieved which eliminated many of the problems associated with alternating current techniques. Glass capillaries were not used; rather, nearly any convenient cell diameter would be feasible. The use of large diameter tubes minimized errors which would otherwise arise from the conductivity of glass itself and from cell constant deviations caused by attack of small diameter tubes by the melt under investigation. Furthermore, the direct current circuits employed were considerably more simple to build and operate than corresponding alternating current circuits.

It was shown that the experimentally determined cell constants of the conductivity cells used were very nearly the same as were calculable from cell geometry. Presumably, the constants were identical within the errors of measuring cell dimensions. Within the ranges investigated, conductivities determined in this work were independent of cell current (up to a 40-fold variation). The cell design chosen was simple; no particular difficulties would be encountered in building the cells by anyone possessing moderate glass blowing abilities.

The direct current conductivity of hydrochloric acid

solutions was measured. It was shown that to within one to three parts per thousand the suspected chain mechanism of hydrogen ion conductivity displayed no frequency effect. That is, the present values agreed with published alternating current values.

The direct current conductivities of $LiNO_3$, $NaNO_3$, KNO_3, and their binary mixtures were determined. Agreement with published alternating current values, where available, was excellent. The three binary systems all displayed moderate negative deviations from additivity of specific and equivalent conductivity. The most interesting feature observed for these melts was the minimum in $LiNO_3$-$NaNO_3$ equivalent conductivity isotherms. Lack of experimental data and of a workable fused salt theory precluded satisfactory explanation of equivalent conductivity minima.

Finally, some exploratory experiments were described in which attempts were made to use extremely simple but highly polarizable, highly irreversible reference electrodes in direct current conductivity measurements. The results were encouraging.

PART II. A CARBON DIOXIDE FORMATION CELL

INTRODUCTION AND LITERATURE SURVEY

An electrochemical cell in which the net reaction occurring represented only the consumption of oxygen and carbon and the production of carbon dioxide would have significance in two areas. First, such a device would have fundamental importance in fuel cell research. Secondly, such a cell would provide the possibility of direct determination of the thermodynamics of formation of carbon dioxide. The present research describes several aspects of a carbon dioxide formation cell.

A general discussion of fuel cells and of fuel cell research is much too broad a topic for treatment here. Extensive study in this area is currently underway and an enormous amount of published material is available. The reader is referred here only to two introductory, non-specialized accounts (37,38).

A particularly attractive fuel cell would be one utilizing atmospheric oxygen at the cathode and carbon (from fossil fuels) at the anode. Electrode reactions may be written generally as

$$O_2 + 4e^- \rightarrow 2[O^=] \qquad \text{cathode reaction}$$

$$\underline{C + 2[O^=] \rightarrow CO_2 + 4e^-} \qquad \text{anode reaction}$$

$$C + O_2 \rightarrow CO_2 \qquad \text{net cell reaction}$$

where $[O^=]$ represents some form of solvated oxide ion. This type of fuel cell was first and most thoroughly studied by

Baur and co-workers (39,40,41,42,43,44,45). (Earlier related work has been reviewed by Baur and Tobler (46).) Their research was directed chiefly toward the ultimate development of workable fuel cells. Accordingly, their electrodes and electrolytes were considerably more robust, but less amenable to quantitative treatment, than those which were employed in the present work. Baur tended to prefer electrodes and electrolytes consisting of various metallic oxides and coke in the form of powders bound by borax or soft glass. The cells were operated at temperatures sufficiently high to render the binders fluid and electrically conductive.

Baur and co-workers were able to achieve several promising cells. They did find one serious disadvantage of the carbon cell. That is the necessity of high-temperature ($> 800°$) operation in order to achieve reasonably rapid carbon oxidation (as would be required to draw usefully large current from the cell). Even if one were willing to tolerate the problems of containment and thermal insulation, much of the efficiency of the cell would be lost in non-useful consumption of fuel through the equilibrium

$$C + CO_2 = 2CO$$

The equilibrium lies well to the right at high temperatures, but it was observed in the present work that it was rather slowly attained. Several low-temperature carbon cells were investigated and are described below; however, no attempt was

made to devise an experimental low-temperature fuel cell prototype.

Any electrochemical cell (of which $C,CO_2/electrolyte/O_2$ is an example) for which the net reaction is the formation of a compound from its elements may be termed a formation cell (47). If the cell is equipped with reversible electrodes, and if junction or diffusion potentials are absent or negligible, then one can calculate the free energy, ΔG, enthalpy, ΔH, and entropy, ΔS, of formation of the compound under the prevailing temperature and pressure. The necessary equations for a constant pressure process are as follows:

$$\Delta G = -nFE$$

$$\Delta H = -nF\left(E - T\frac{dE}{dT}\right)$$

$$\Delta S = nF\frac{dE}{dT}$$

where

n = the number of electrons transferred in the net cell reaction

F = the faraday

T = absolute temperature.

It is often true that formation cells can furnish more reliable molar and partial molar thermodynamic data than can the more usual thermal and cryoscopic methods. A number of such cells have been studied in fused salt media; however, the lack of reversible cathodes has largely restricted such

work to halides. Murgulescu and Sternberg (47) recently have reviewed halide investigations. Rose, Davis and Ellingham (48) have summarized some of the work with oxide formation cells, and also have presented some of their own findings on halide, oxide, and sulfide cells.

Some of the earliest work with metal oxide formation cells was done by Treadwell (49). His electrolytes consisted of the powdered metal oxide under investigation, mixed with a little borax. He used a liquid silver cathode through which oxygen was bubbled. Most of the recent work with oxide formation cells has involved platinum, oxygen electrodes. Mashovets and Revazyan (50) have studied various reactions of aluminum in cryolite-alumina melts. Hill, Porter and Gillespie (51) have investigated the formation of iron, nickel, and copper oxides in metal oxide saturated Li_2SO_4-K_2SO_4 melts. Delimarskii and Andreeva (52,53) and Delimarskii and Nazarenko (54) measured formation voltages and activities of PbO and Bi_2O_3 in the pure oxide melts and in oxide-$NaPO_3$ and oxide-$Na_2B_4O_7$ melts.

In the present research, the following formation cell was studied:

$$C_{graphite}, CO_2/\text{fused salt electrolyte}/Pt, O_2.$$

The most frequently used electrolyte was a mixture of Na_2WO_4 (85 weight %) and WO_3 (15 weight %). This composition was not far removed from the eutectic mixture which melts at 626°

(55). Some studies were carried out in chromate, sulfate, and borate melts and in dilute hydroxide and carbonate melts. Duke and Copeland (56) have conducted some exploratory research with borate and tungstate systems.

Since processes occurring at the carbon electrode were of primary interest in this work, it was important that a reliable oxygen electrode be used. Reversible oxygen electrodes apparently are very nearly unavailable for use in aqueous systems (57), but they can be devised for use at the higher temperatures commonly encountered in salt melts. Electrodes reversible with respect to oxygen gas and oxide ion are most frequently simply a noble metal surface over which oxygen gas is bubbled. Gold, silver, and a few less inert metals have been used, but platinum seems to be the most versatile choice.

Baur and Brunner (42), Janz and Saegusa (58), Janz and Colom (59), and Stepanov and Trunov (60) have studied Pt,O_2 electrodes in alkali metal carbonates. The latter authors (60) observed the electrode to be reversible so long as a carbon dioxide partial pressure greater than the carbonate dissociation pressure was maintained in the oxygen stream. Flood, Förland and Motzfeldt (61) employed Pt,O_2 electrodes (with CO_2) in Na_2CO_3-Na_2SO_4 melts. Hill, Porter and Gillespie (51) and Flood and Förland (62) worked with alkali sulfate melts. It was reported (51) that iron poisoned the

platinum surface, and a method to remove iron was worked out. Lux (63) also used sulfate melts with Pt,O_2 electrodes, but felt that Au,O_2 electrodes were superior.

Csaki and Dietzel (64), Delimarskii and Nazarenko (54), Delimarskii, Andreeva and Nazarenko (65), and Nazarenko (66) constructed concentration and formation cells which involved Pt,O_2 electrodes in $Na_2B_4O_7$ melts. Delimarskii and Andreeva (52,53,67) built similar cells employing an electrolyte of $NaPO_3$. Other melts have been studied. These include lead silicate (68), cryolite-alumina (50), and sodium hydroxide (48,69). Kust (70), Shams El Din (71), and Shams El Din and Gerges (72) very recently have developed Pt,O_2 electrodes for use in alkali nitrate systems. Kust found the electrode to be completely reversible; this is perhaps the lowest temperature system so far reported wherein oxygen electrode reversibility is attainable.

The consensus of the authors cited above appears to be that Pt,O_2 electrodes are reversible so long as no significant current drain occurs. Some investigators actually tested for reversibility; others reported no evidence of a lack of reversibility. In one case, non-reversibility was claimed; Flood, Förland and Motzfeldt (61) reported that Pt,O_2 electrodes did not behave properly in a K_2CrO_4-$K_2Cr_2O_7$ melt.

In view of the generally satisfactory properties of

Pt,O_2 electrodes (at least, in oxy-anionic melts), they were employed in the present research.

Both anodic and cathodic oxygen electrode overpotentials have been studied, but the number of such investigations is limited. Flood and Førland (62), Karpatscheff and Patzug (73), and Janz and Colom (59) have measured anodic overpotential in, respectively, sulfate, nitrate, and carbonate melts. Cathodic overpotential in carbonate melts was studied by Baur and Brunner (42). Agar and Bowden (69) studied both anodic and cathodic overpotentials of platinum in fused NaOH. Platinum-oxygen electrode overpotentials also were measured in the present research.

Considerably less information is available on carbon, carbon dioxide electrodes. Of course, Baur used carbon electrodes in his fuel cell work, which has already been mentioned. His electrodes were of a type quite different than those employed in the present study, and will not be discussed here. What other work has been done was published in various Russian journals, and has been summarized in a book by Delimarskii and Markov (74). The various investigators reported that carbon electrodes (bathed in CO_2 and/or CO) behaved as oxygen-oxide electrodes when immersed in oxy-anionic melts. Assuming the equilibria

$$CO_2 + C = 2CO$$

and

$$CO_2 = CO + \tfrac{1}{2}O_2$$

exist at the carbon surface, this is equivalent to saying that carbon functions as a CO_2 electrode (or as a CO electrode).

Graphite rods, over which CO_2 and/or CO was bubbled, served as anodes in the present research. Studies were made of cathodic and anodic overpotentials at the graphite electrodes.

EXPERIMENTAL

Materials and Equipment

Chemicals

"Baker Analyzed" K_2SO_4, K_2CrO_4, Na_2CO_3, and NaOH and North Metal and Chemical Co. (York, Penna.) C. P. grade WO_3 all were used without further purification. "Baker Analyzed" $Na_2Cr_2O_7 \cdot 2H_2O$, $Na_2B_4O_7 \cdot 10H_2O$ and $Na_2WO_4 \cdot 2H_2O$ all were oven-dried to the corresponding anhydrous salts. "Baker Analyzed" H_3BO_3 was heated for a prolonged period at 500-600° (until well after bubbling ceased) in order that anhydrous B_2O_3 might be obtained. Before each experiment in which it was used, "Baker Analyzed" potassium pyrosulfate was heated for several hours at the maximum temperature to which it was to be subjected in the experiment. During the heating period, the salt was under aspirator vacuum.

Cylinders of argon (Newkirk Sales and Service, Waterloo, Ia.), carbon monoxide (C.P. grade; The Matheson Co., Inc., Joliet, Ill.), carbon dioxide (Mitcheltree Fire Extinguisher Co., Des Moines, Ia.), and oxygen (U.S.P. grade; Wright Welding Co., Des Moines, Ia.) were required. The oxygen was passed through a $Mg(ClO_4)_2$ drying tower and used without further purification.

A gas train was set up for purification of CO, CO_2, Ar, and mixtures of these gases. After passing through a $Mg(ClO_4)_2$

drying tower and a flow meter, each gas was led into a helical mixing chamber. From this chamber the gas (or gas mixture) passed through a tube heated to 500° and containing copper powder, thence through a tube, also heated to 500°, containing cupric oxide powder. Finally, the gas flowed through a tube filled with Ascarite and more $Mg(ClO_4)_2$. The cupric oxide and Ascarite tubes were provided with by-passes so that a gas which would otherwise be absorbed could be supplied to the electrochemical cell.

By appropriate operation of the purification train, CO_2-free CO and CO-free CO_2 could be obtained. All gases were oxygen-free. On occasion exceptionally pure argon was desired. In such instances the tube containing copper powder was replaced by a tube filled with tantalum chips and heated to 800°.

Furnaces

Various tube furnaces were used to heat cells. These furnaces were mounted vertically and had suspended in them large test tubes containing the fused salt solutions under investigation. During the course of the research three different temperature controllers were used. These were a Bristol "Model 536 Indicating Electronic Pyrometer Controller" (The Bristol Company, Waterbury, Conn.) and two Honeywell proportional controllers (Minneapolis-Honeywell Regulator Co., Philadelphia, Penna.). One of the Honeywell controllers

actuated a servo-motor which in turn varied the setting of the furnace Powerstat. The other two controllers merely switched furnace current on and off. In all cases, melt temperature could be held to a one degree variation once thermal equilibrium was reached. Chromel-alumel thermocouples, located in air and near the fused salt containers, led from furnace to controller.

Most of the furnaces used had no provision for adjustment of temperature gradient within the furnace cavity. In all experiments, fused salt containers were of relatively large cross section and contained shallow melts; convection within the containers was relied upon to provide uniform temperatures within all regions of the melts.

Temperatures within the electrochemical cells were measured by a Leeds and Northrup Model 8662 thermocouple potentiometer. The potentiometer was provided with a reference junction correction slidewire. Chromel-alumel thermocouples were used. Hot junctions were sheathed in quartz or Vycor, and were immersed in the fused salt solutions.

Electrochemical cells

All cells used were basically alike in that they consisted merely of a large test tube (from 38 to 54 mm I.D.) suspended in a furnace and containing the salt under investigation. Immersed in the melt were two electrodes. The electrodes were physically isolated from one another by

placing one of them within a second, smaller, test tube which had a very small hole in the bottom through which electrical contact was made. For experiments in which current was passed through the cell, one or more reference electrodes also were employed. Since the reference electrodes were identical to the working electrodes, each reference electrode was located immediately adjacent to its corresponding working electrode.

All gas electrodes were of the same basic design and provided a means to pass fresh gas over the immersed surface of platinum or graphite. Typical platinum, oxygen and graphite, carbon dioxide electrodes are shown in Figure 6. It usually was the graphite, carbon dioxide electrode which was placed within the smaller test tube electrode compartment. In order to exclude air from the compartment, its upper end terminated in a 34/45 outer joint. The corresponding inner joint (shown in Figure 6) closed the compartment. When a graphite reference electrode was used, a different 34/45 inner joint was employed; this joint was provided with two electrodes, both of the same type as is shown in the Figure.

Use of platinized platinum foil instead of shiny platinum wire did not appear to be advantageous. Neither did prior "soaking" of the electrode in the melt under investigation affect experimental results. Whether or not the graphite electrode-platinum lead junction was above or below the

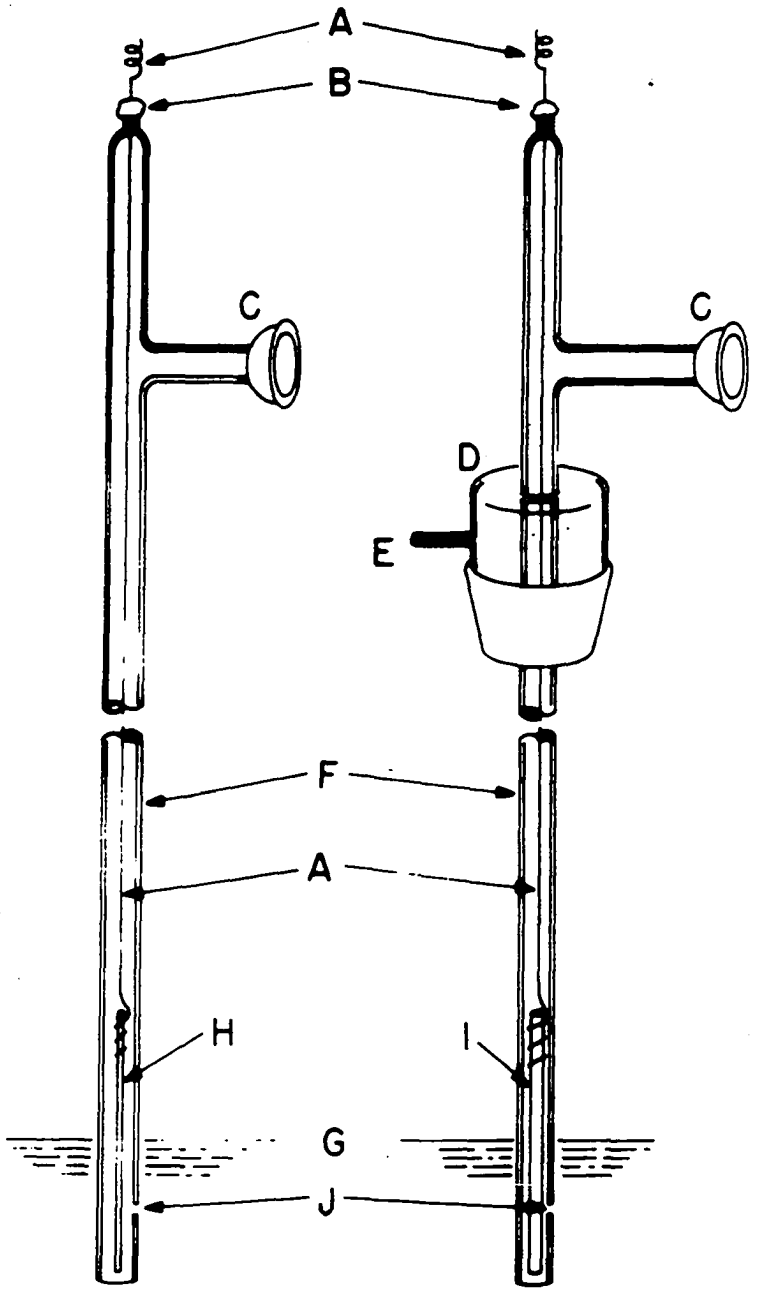

A - PLATINUM LEAD
B - WAX SEAL (APIEZON T)
C - 18/7 VYCOR SOCKET (GAS INLET)
D - 34/45 VYCOR JOINT
E - GAS OUTLET
F - 7mm ID VYCOR
G - LEVEL OF MELT (APPROXIMATE)
H - 1/16" DIA. PLATINUM WIRE
I - 0.120" DIA. GRAPHITE ROD
J - 2mm HOLE

Figure 6. Typical platinum, oxygen and graphite, carbon dioxide electrodes

surface of the melt in the carbon electrode compartment was of no significance. The platinum-graphite interface apparently did not serve as a preferred reaction site, nor was any large thermal emf generated. The latter statement was independently confirmed by determining thermal emf in a separate experiment. It is also worthwhile mentioning that platinizing the graphite itself offered no benefits.

National Carbon Company spectrographic grade graphite rods were used as electrodes in this work.

Most of the experiments which were performed involved Na_2WO_4-WO_3 melts. These melts appeared to very slowly attack both Vycor and fused silica. The cells could be used for periods up to several weeks without seepage or serious attack; however, glass invariably broke when cooled, no matter how briefly it had been exposed to the melt. It was necessary to use some container other than glass to hold $Na_2B_4O_7$-B_2O_3 melts. Large nickel crucibles were satisfactory. Glass electrodes and electrode compartments could be used for periods of a few days without disintegration, so long as no appreciable mechanical stress was put upon them. Carbonate- or hydroxide-containing melts presented serious containment difficulties. Containers such as platinum or gold were unavailable and, in any case, would have been unsuitable for electrode construction. In practice, nickel and glass were used and experiments were completed within a few hours. The

other melts studied presented no containment or corrosion problems.

Electrical Measurements

Cell voltage

Cell voltages were measured in three different ways as work progressed. A conventional potentiometric circuit was employed for preliminary experiments and for all runs with other than tungstate melts. A Leeds and Northrup type K-3 potentiometer and type 2430A galvanometer were used.

It became evident that even the small currents necessarily passed through the cells when searching for the galvanometer null point tended to polarize the electrodes slightly. While it was possible to arrive eventually at meaningful emf values, the time required to do so would have been intolerably long in experiments designed to study the variation of electrode polarization with cell current. Accordingly, electrometers were acquired. (Keithley Instruments, Inc. models 600A and 603 were used. For the purposes of this research, the two electrometers were identical in operation and characteristics and no distinction will be made between them hereafter.) According to the manufacturer's specifications, electrometer input impedance was greater than 10^{14} ohms. It was therefore assumed that any electrode polarization caused by current drain through the electrometer

would be completely negligible. No experimental evidence to refute this assumption was found.

The electrometer was used in place of a galvanometer as the null indicator of a potentiometric circuit for those experiments in which "open circuit" cell voltages were sought. For those experiments in which electrode overpotential was studied as it depended upon cell current, a slightly different measurement technique was used. The electrometer and a potentiometer were placed in series with a reference electrode and the electrode under investigation. The potentiometer supplied a potential of equal magnitude and opposite polarity to the emf developed between the reference electrode and investigated electrode at zero cell current. As cell current increased from zero, the voltage indicated by the electrometer was identically the electrode overvoltage. Bucking potentials on the order of a few millivolts were required between any two graphite electrodes. Normally any two platinum electrodes were sufficiently reversible that no bucking potential at all was necessary.

Electrode overvoltage

A 6-volt storage battery supplied polarizing currents. The battery was connected in series with a multirange ammeter, a resistance variable down from 22-megohms, and the Pt,O_2 and C,CO_2 electrodes. By simply reversing battery polarity, one could measure overpotential when the cell was operated in

either normal or reverse direction. When the cell was operating normally, it made no difference in the observed overpotential at any given current whether the battery was used as a current supply or the cell was simply shorted by a resistor. Because of its greater convenience, the battery was nearly always used.

On occasion the rate of growth or decay of overpotential was of interest. A Moseley X-Y recorder was used to record overpotential variations occurring from five to several hundred seconds after the polarizing current was turned on. The X-axis signal was provided by the electrometer output terminals. An internal time base supplied the Y-axis signal. A Tektronix, Inc. type 545A oscilloscope (with type CA plug-in dual trace preamplifier) was used to follow overpotential changes which occurred in less than five seconds from onset of polarizing current. Oscilloscope traces were recorded on Polaroid ASA 3000 film with a "Beattie Oscillatron" model KLLP type 12445 camera (Beattie-Coleman, Inc., Anaheim, Calif.). As before, an internal time base and the electrometer output provided signals to the oscilloscope. A double pole switch in the polarizing current supply circuit simultaneously switched on (or off, as appropriate) cell current and triggered the oscilloscope trace.

RESULTS AND DISCUSSION

Cell Voltage

It is easy to calculate the theoretically expected voltages for the cell

$$C_{graphite}, CO_2/electrolyte/Pt, O_2.$$

From the free energy functions and the constants, H_o°, as tabulated in Lewis and Randall's book (75), the standard electromotive force of the formation cell was calculated to be 1.026 volts over the temperature range of this research. If carbon dioxide is passed over a graphite surface sufficiently slowly, it will react to establish the equilibrium

$$CO_2 + C = 2CO.$$

Accordingly, the equilibrium constant also was calculated at a number of temperatures, and from these values, the partial pressure of CO_2 at each temperature was obtained. (It was assumed that $f_i = p_i$ and $\Sigma\, p_i = 1$, where f_i and p_i are, respectively, the fugacity and partial pressure of gas i.) It was then possible to calculate the temperature dependence of the theoretically expected voltages from the equation

$$E_T = E^\circ - \frac{RT}{4F} \ln \frac{P_{CO_2}}{P_{O_2}}$$

where

E_T = theoretically expected voltage at temperature T

E° = standard voltage

R = the gas constant

T = absolute temperature

F = the faraday

P_{O_2} = partial pressure of oxygen at the oxygen electrode (assumed to be unity).

Figure 7 shows E° and E at various temperatures. It should be noted that E, as calculated above, also is identically the voltage one expects from the following cells:

$$C_{graphite}, CO(P_{equil})/electrolyte/Pt, O_2(p=1)$$

and

$$C_{graphite}, O_2(P_{equil})/electrolyte/Pt, O_2(p=1)$$

where the pressures of CO and O_2 at the graphite are those computed from the simultaneous equilibria

$$C + O_2 = CO_2$$

$$CO_2 + C = 2CO$$

$$CO_2 = CO + \tfrac{1}{2}O_2.$$

The equilibrium partial pressure of all three gases are shown in Figure 8.

Various electrolytes were tried and are indicated in Table 5. Also shown in the table are the maximum voltages obtained in each melt at one or more typical temperatures. All experiments in melts other than the tungstate system must be considered as exploratory, for no particular effort was made in such cases to improve upon the results obtained.

The very low voltages observed in the first three melts

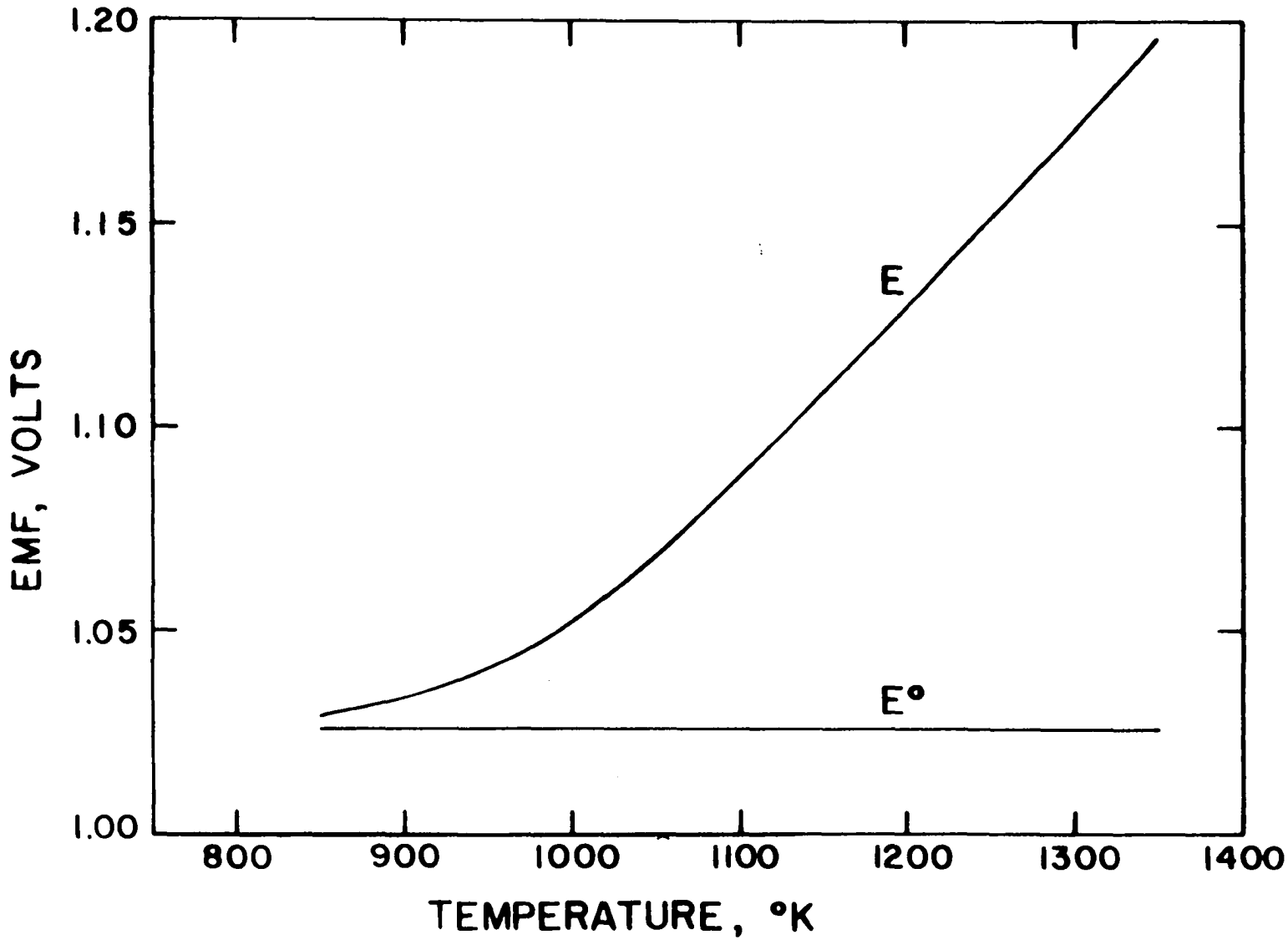

Figure 7. Calculated voltages for the cell C(gr),CO_2/ electrolyte/Pt,O_2

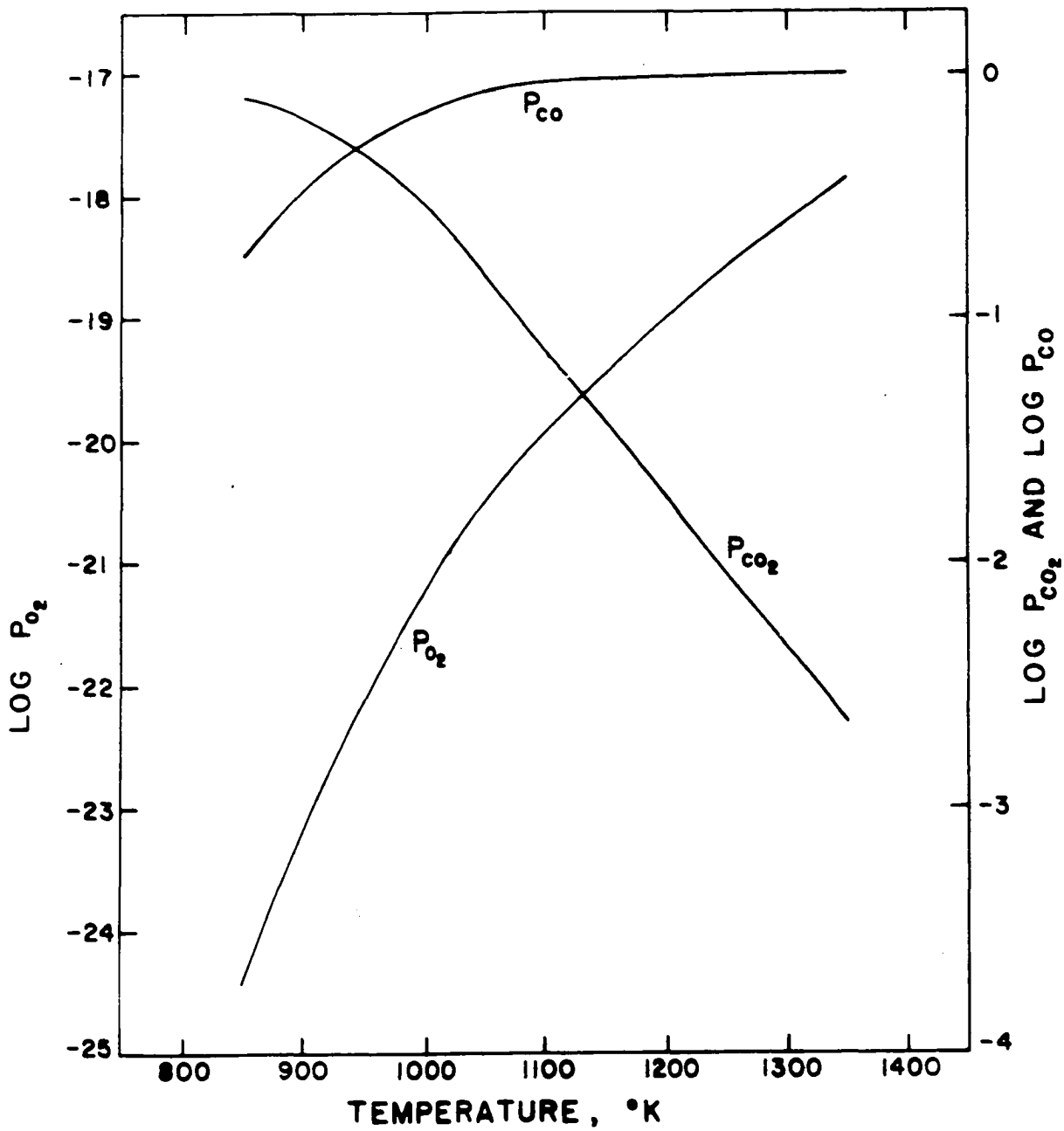

Figure 8. Equilibrium partial pressures of oxygen, carbon monoxide and carbon dioxide on graphite

Table 5. Electrolytes employed in CO_2 formation cells

Electrolyte	Temperature, °C	Maximum emf, volts
K_2CrO_4-$Na_2Cr_2O_7$	400	0.13
	500	0.1
K_2CrO_4-$Na_2Cr_2O_7$-NaOH	400	0.5
K_2SO_4-$K_2S_2O_7$	400	0.3
B_2O_3-$Na_2B_4O_7$	800	1.04
	850	1.06
	860	1.08
B_2O_3-$Na_2B_4O_7$-Na_2CO_3	800	.95
WO_3-Na_2WO_4	800	.90

indicated in the table were not unexpected. The hydroxide and pyrosulfate melts were not thoroughly dry. Furthermore, water was generated as CO_2 came into contact with NaOH. A green deposit, presumably Cr_2O_3, was formed on the interior walls of the graphite electrode compartment in experiments which used the chromate-dichromate system. Duke and Copeland (56) also noted reduction of the melt in their experiments in a MoO_3-Na_2MoO_4 system. In that instance, metallic molybdenum deposited on the graphite.

Borate systems ostensibly were the most promising of the melts tried, in that cell voltages very nearly equalled the theoretical values. It is also true that there is no possibility of chemical oxidation of graphite by a borate

melt. On the other hand, severe disadvantages of such melts were evident. Silica was completely unsatisfactory as a container, and was not especially suited for electrode and electrode compartment construction. The viscosity of such melts is extremely high, and led to difficulty in obtaining satisfactory operation of the gas electrodes employed. Overvoltage of these cells was very much higher than was observed in tungstate melts. If the overvoltage was caused primarily by concentration gradients in the vicinity of the electrodes, then its magnitude also could be attributed to the high viscosity of the borate system.

Most of the present work was performed with WO_3-Na_2WO_4 electrolytes. It has already been mentioned that the tungstate systems offered no containment difficulties. Their viscosities were sufficiently low to permit satisfactory gas electrode operation. Furthermore, it was possible to vary WO_3 content from zero to about 70 mole % and still not exceed a 750° melting point (55).

The platinum, oxygen electrode performed satisfactorily in tungstate melts, and was assumed to be reversible. Cell voltage changed very nearly as would be calculated from the Nernst equation when air was substituted for oxygen at the oxygen electrode. This behavior also was noted by Duke and Copeland (56). Approximately correct voltages were observed from the cell

$W/WO_3\text{-}Na_2WO_4/Pt,O_2$.

The standard voltage of this cell was calculable from thermodynamic data (24) but, since activity of WO_3 was unknown, the actual voltage to be expected could be estimated only.

Interpretation of the electrochemical behavior of the graphite electrode in tungstate melts was equivocal. The relatively small amount of published information on graphite anodes in oxy-anionic melts (74) indicates that graphite, bathed in CO_2 or CO, behaves as an oxygen electrode. A more detailed discussion of this concept will follow below.

Figure 9 shows the temperature dependence of cell voltage as observed in a typical experiment. Cell voltages were not very reproducible from one experiment to another, but always the same general form of the temperature dependence was found. At any given temperature in the same melt, cell voltage fluctuated from day to day by as much as 10 to 20 millivolts. Since no uniform trend in the variations was observed, the reason for such behavior was not clear.

Cell voltage was also dependent upon the composition of the tungstate melts. Data are presented in Figure 10 for two experiments in which increasing amounts of WO_3 were added to initially pure Na_2WO_4 melts. The data for each of the experiments were all collected within a 12-hour period. Except as otherwise indicated below, all experiments in tungstate melts were performed on melts of the composition

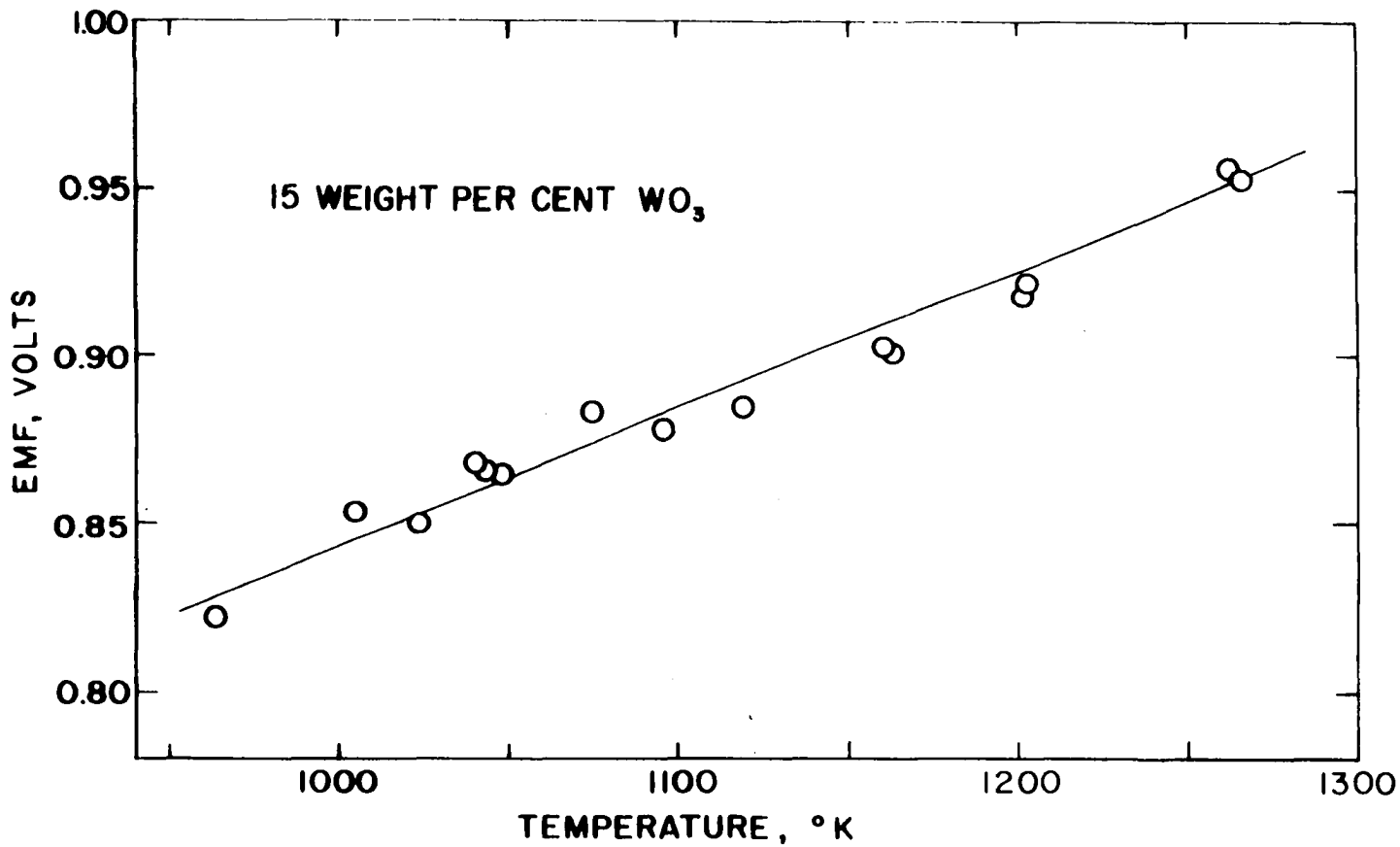

Figure 9. Temperature dependence of cell voltage

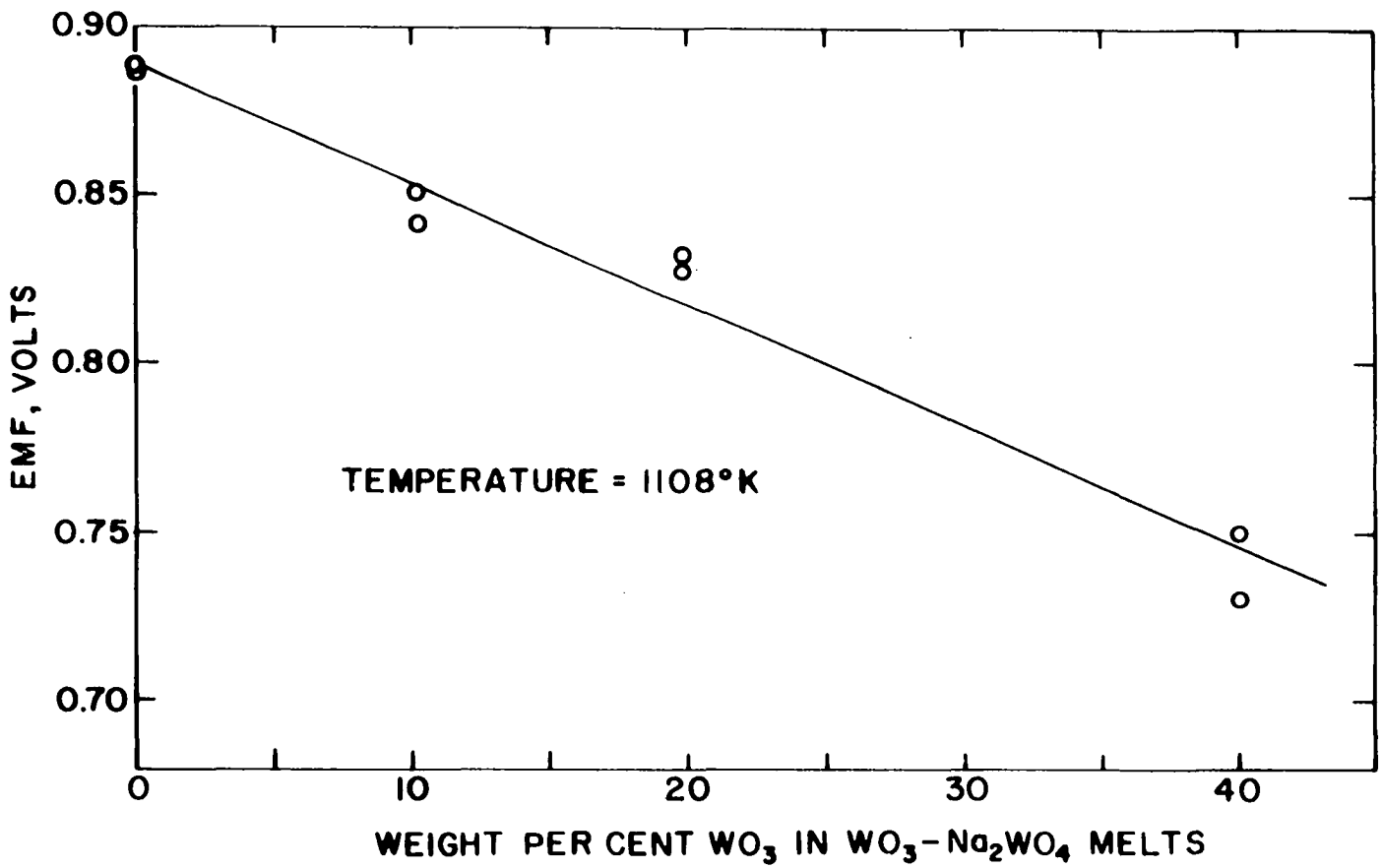

Figure 10. Dependence of cell voltage on melt composition

15 weight % WO_3, 85 weight % Na_2WO_4. This composition is nearly the eutectic mixture, and was chosen to permit a wide temperature range of operation.

Graphite anodes apparently were not reversible in tungstate melts. Cell voltages were highly dependent on CO_2 flow rate, the voltage decreasing with increased flow rate. The voltage relationship was nearly logarithmic in flow rate. Plots of cell voltage vs. log flow rate at different input CO_2 partial pressures (the diluent was argon) gave a family of lines of approximately the same slope. Similar behavior was observed when carbon monoxide was the electrode gas. When the electrode gases were passed through a furnace containing graphite heated to the temperature of the electrochemical cell, then introduced to the graphite electrode, the flow rate dependence of voltage was less pronounced. This effect was interpreted as implying that the establishment of the equilibria involving graphite, CO_2, CO, and O_2 was relatively slow. If the equilibria are, indeed, slowly attained, fuel depletion in a graphite-air fuel cell through the reaction of CO_2 with graphite might not be as serious as has been thought.

Further evidence of slow attainment of the equilibria may be cited. Argon was bubbled over a large (95 cm^2) graphite anode and the effluent gases were passed through a gas train so that CO_2 and CO (oxidized by CuO to CO_2) could

be collected and weighed. The argon was first freed from oxygen by being passed over hot tantalum. A known amount of current was passed through the cell and was measured with a copper coulometer (76). (The number of equivalents of gas collected agreed to within 5% of coulometer values.) Zero-current blank determinations were run at each temperature. Results of this experiment are presented in Table 6.

Table 6. Gas formation from a graphite-oxygen electrochemical cell

Temperature, °K	Current, milli-equiv.	(CO_2/CO), blank	(CO_2/CO), electro-chem.	Current density at anode, ma cm^{-2}
1027	20.2	9.6	29.3	3
1139	23.2	1.5	11.9	4

Two conclusions may be drawn from the observation that at each temperature the electrochemical CO_2:CO ratio exceeded the blank ratio. First, the equilibrium between CO_2 and CO must have been established rather slowly, for if not, the ratios should be identical. Secondly, such large ratios suggest that CO_2 was the primary electrochemical product, and not CO.

A few experiments were performed in which a constant electrode gas flow rate was maintained as the partial pressure of CO_2 was changed. The Nernst equation was not obeyed. Voltage changes were very much smaller than the

theoretical effect, and plots of emf vs. log p_{CO_2} were sharply concave toward the log p_{CO_2} axis.

It is appropriate at this point to make some preliminary remarks concerning the reactions suspected of occurring at the anode. It can be calculated from thermodynamic functions (24,75) that the standard free energies of the reactions

$$2/3\ WO_3 + C \longrightarrow 2/3\ W + CO_2$$

and

$$2\ WO_3 + C \longrightarrow 2\ WO_2 + CO_2$$

are negative at temperatures in excess of 980 °K and 870 °K, respectively. If the assumption is made that graphite is functioning as an oxygen electrode, an approximation can be derived for cell voltage expected when oxygen partial pressure is governed by each of the equilibria

$$WO_3 = W + 3/2\ O_2$$

and

$$WO_3 = WO_2 + 1/2\ O_2.$$

The voltages are shown in Figure 11. That the voltages are only approximations is evident from the fact that WO_3, WO_2, and CO_2 are not present at unit activity.

The experimentally observed cell voltages, such as are presented in Figures 9 and 10, must be reconciled with the curves of Figure 11 if the assumption that graphite behaved as an oxygen electrode is to be justified. The negative slope of the curve shown in Figure 10 is what would be

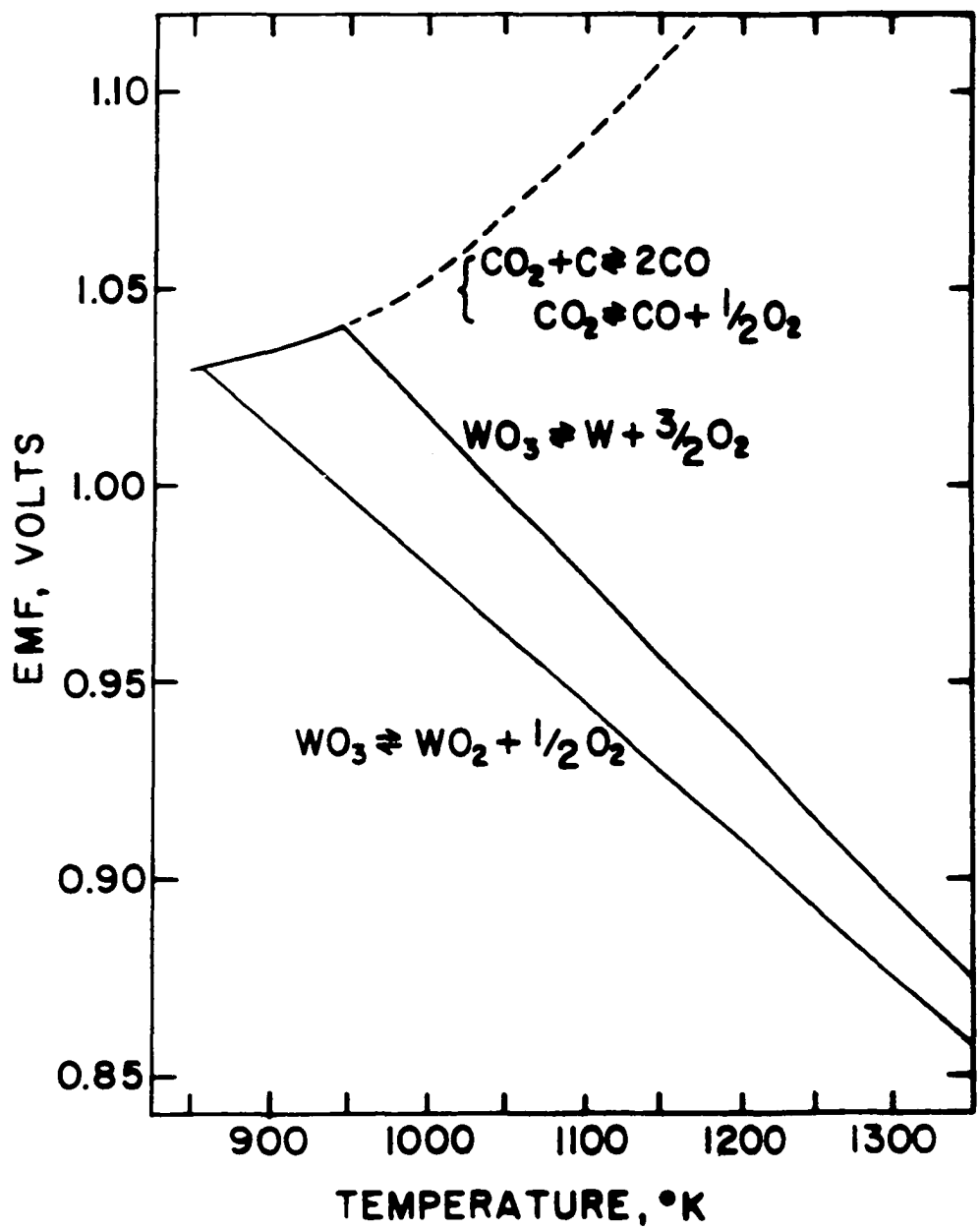

Figure 11. Cell voltages calculated for graphite, oxygen anode

expected if dissociation of WO_3 governed the oxygen partial pressure seen at the graphite-melt interface. The positive slope of the curve of Figure 9 is more difficult to explain. The data represented by Figure 9 all were taken at some constant CO_2 flow rate. It has been shown that gas equilibria involving graphite are sufficiently slowly attained that a flow rate voltage dependency could be observed. As temperature is raised, such equilibria would be established more and more rapidly at any constant flow rate. The incoming electrode gas was freed from oxygen by passage through a gas train which included heated tubes of Cu and CuO. The equilibrium partial pressure of oxygen over CuO at 500° is several orders of magnitude greater than the equilibrium pressure at a graphite-WO_3 interface. Therefore, to the extent that the latter partial pressure equilibrium remained unestablished, cell voltage would be below the expected value. As the temperature of the electrochemical cell was increased, the partial pressure of oxygen would more nearly approach the calculated value, and cell voltage would increase. Since WO_3 activity was not unity, cell voltages greater than those shown by Figure 11 were not surprising.

Further examination of the ideas just presented awaits a gas purification train capable of providing electrode gas of a lower oxygen content.

An alternate mechanism can be proposed to explain the

deviations of cell voltages from the theoretical values. This mechanism does not necessarily presuppose reversibility of electrodes; indeed, it rejects the idea. Let it be assumed that graphite reacts with the melt to form a very thin layer of tungsten bronze at the graphite-melt interface according to an equation such as

$$2xNa^+ + 2WO_4^= + C \longrightarrow 2Na_xWO_3 + CO_2 + (4-2x)e^-$$

where x is a number less than one. The value of x undoubtedly is influenced by the WO_3:Na_2WO_4 ratio of the melt in the immediate electrode vicinity and probably also is affected by the kinetics of bronze formation. Tungsten bronzes are insoluble in tungstate melts, and presumably would remove graphite from a potential-determining role. A secondary cell then would exist, with emf determined by the composition of the tungsten bronze.

Passage of current through such a cell would electrochemically reoxidize Na_xWO_3 to Na_2WO_4, whereupon a new bronze layer would be formed. The complete cell is describable by the sequence of reactions

$$2xNa^+ + 2WO_4^= + C \longrightarrow 2Na_xWO_3 + CO_2 + (4-2x)e^- \quad \text{at anode}$$

$$2Na_xWO_3 + 2[O^=] \longrightarrow 2xNa^+ + 2WO_4^= + 2xe^- \quad \text{at anode}$$

$$4e^- + O_2 \longrightarrow 2[O^=] \quad \text{at cathode}$$

$$C + O_2 \longrightarrow CO_2 \quad \text{net cell reaction}$$

Unfortunately, there is insufficient thermodynamic data available on tungsten bronzes to discuss further the merits of

this proposal in terms of the experimental data which were obtained.

Electrode Overpotential

Overpotential of an electrochemical cell may be defined by the equation

$$\eta_I = E_I - E_r$$

where

η_I = overpotential at current I

E_I = cell voltage at current I

E_r = reversible cell voltage at zero current.

One may investigate the overpotential of a single electrode by following the cell current dependence of the voltage between the electrode under study and a "dead" or reference electrode. Often the current density at an electrode surface is of more fundamental importance than is the total cell current. The design of the electrodes employed in the present work precluded knowing current densities; however, the assumption was made that current density was directly proportional to total current.

Electrode overpotential may be defined further by the equation

$$\eta = \eta_O + \eta_A + \eta_C$$

where

η_O = ohmic overpotential

η_A = activation overpotential

η_C = concentration overpotential.

Ohmic overpotential arises from electrical resistance of the cell and is linearly proportional to cell current (Ohm's law). In the absence of oxide or similar films at the electrode surface, η_O is usually small in fused salt systems at all but very large current densities. Ohmic overpotential was measured by means of high speed photography of an oscilloscope screen. The trace was photographed while cell current was on, then again several microseconds to several milliseconds after current was switched off. Cell resistance could be computed from the displacement of the trace. Resistances were well under 10 ohms.

Activation overpotential arises from the energy barrier of a rate-controlling step involved in the cell reaction. Activation overpotential usually obeys the so-called Tafel equation

$$\eta_A = a + b \log I$$

where a and b are experimentally and theoretically derivable constants.

Concentration overpotential arises from concentration gradients of the electrochemically active species in the immediate vicinity of the electrode. Equations describing η_C are presented below.

The type of overpotential experienced by an electrode

may often be identified not only by its current dependence, but also by the manner in which it decays when current is switched off. Ohmic overpotential decays instantaneously. Activation overpotential decays exponentially in time. Concentration overpotential decays slowly and in a complex manner.

Of the many discussions in the literature which are concerned with overpotential, only three will be cited here. Glasstone (8) and Kortüm and Bockris (77) have presented general treatments of overpotential; Agar and Bowden (78) gave a detailed presentation of concentration overpotential.

If the electrochemically active ionic species is not carrying an appreciable fraction of the cell current, and if the active species is diffusing toward the electrode under study, it easily may be shown that

$$\eta = \frac{RT}{nF} \ln \left(1 - \frac{I}{I_\ell}\right)^1$$

where

R = the gas constant

T = absolute temperature

n = number of electrons transferred to or from the electrochemically active species

F = the faraday

I = cell current

[1] Hereafter, η_C will be denoted simply as η.

I_ℓ = a constant; the "limiting" cell current.

If the active ionic species is diffusing away from the electrode, the logarithmic term becomes $\ln(1 + I/I_\ell)$. Both platinum and graphite electrodes, immersed in tungstate melts, were anodically and cathodically polarized. In all four instances, the equations of concentration overpotential were obeyed.

Typical anodic and cathodic polarization curves for a platinum, oxygen electrode are shown in Figure 12.[1] Both curves, and their relative magnitudes, are of the form predicted by the equations for concentration overpotential. They apparently correspond to an ionic species moving toward a platinum cathode and away from a platinum anode. As the cathodic overpotential became large, a second reaction apparently came into prominence. One and sometimes two additional reactions were detectable at even higher overpotentials. None of the subsidiary electrode processes were studied.

The data were analysed by converting the concentration overpotential equations to the form

$$e^{\frac{nF\eta}{RT}} = 1 \pm \frac{I}{I_\ell}$$

---

[1]Except as otherwise indicated, all experiments discussed below were performed in 85 weight % Na_2WO_4, 15 weight % WO_3.

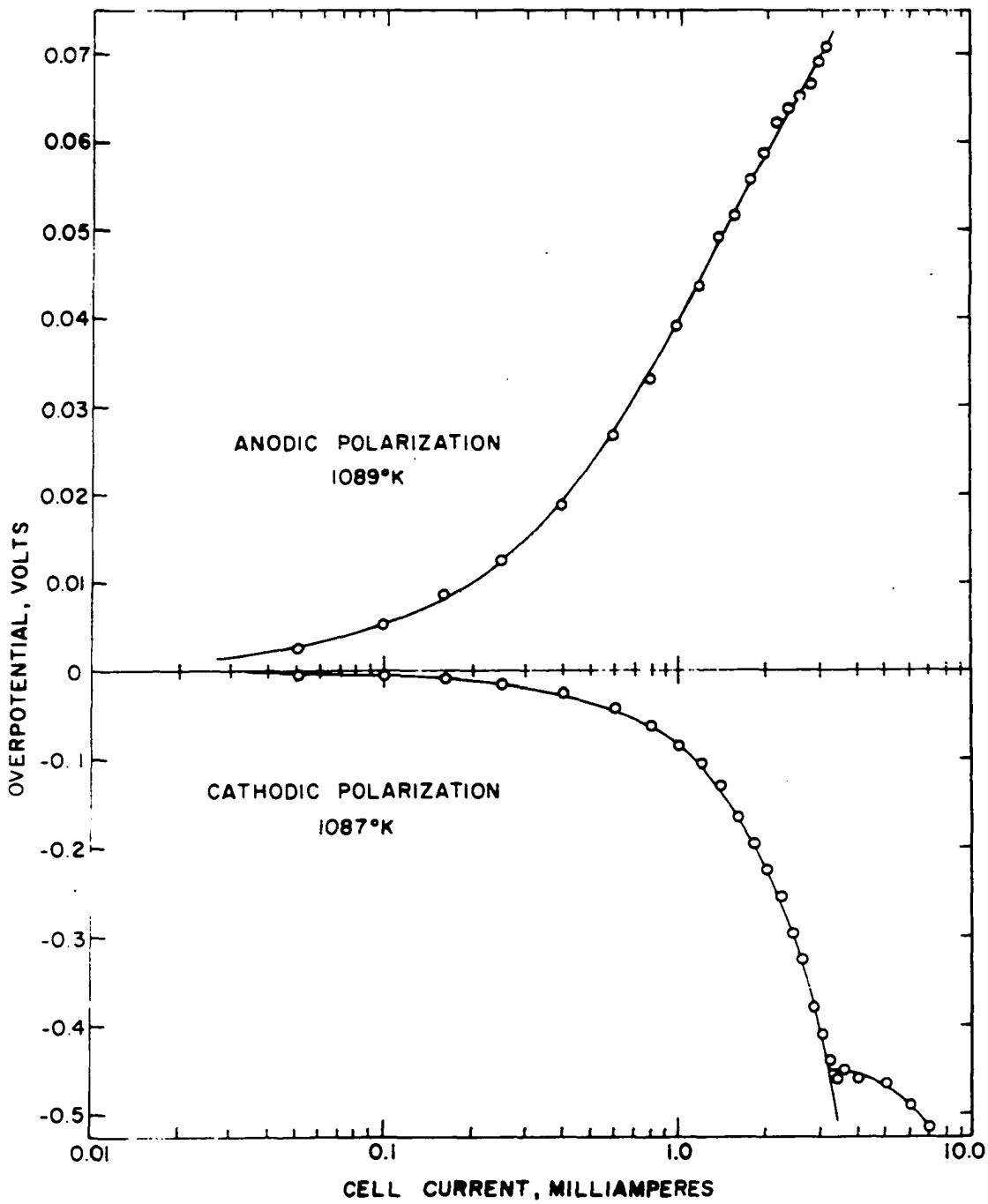

Figure 12. Polarization of platinum, oxygen electrodes

and constructing graphs of the exponential function vs. cell current. Any given set of data was assigned the values n = 1, 2, 3, 4. That value of n for which a straight line was obtained was assumed to be the number of electrons transferred in the rate-determining process. The number of electrons transferred was clearly one for the cathodic process. The anodic polarization curves were less sensitive to the value of n, but unity was strongly indicated. In view of the high operating temperatures of the cell, a value of one for n was not surprising. Indeed, a number less than three reasonably would be anticipated.

Some representative curves for the analysis of platinum cathodic polarization are presented in Figure 13. The temperature dependence of I_ℓ was nearly linear. At a given temperature I_ℓ for the anodic process always was slightly larger than I_ℓ for the cathodic process. For both types of polarization, data taken from the same cell were reproducible to within about 5%.

A brief study was made of the effect of melt composition on platinum polarization. The data are shown in Table 7. No interpretation of the data is offered.

It is of interest to compare the present results for platinum overpotential with the work of others. The only cathodic study amenable to quantitative treatment is that of Agar and Bowden (69). They attributed their overpotential

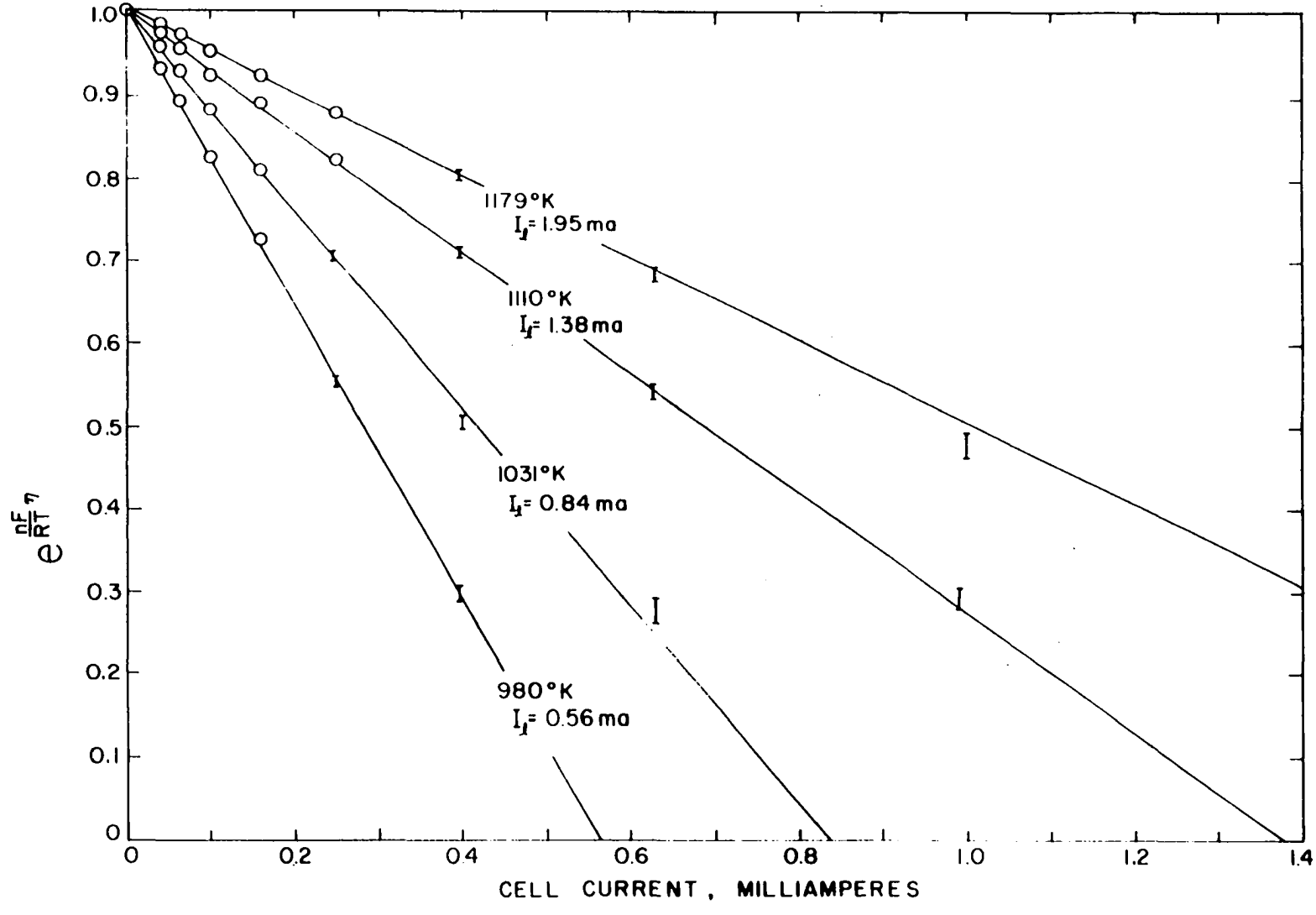

Figure 13. Analysis of platinum cathodic polarization data

Table 7. Dependence of platinum electrode limiting current on melt composition

Type of polarization	Temperature, °K	I_ℓ, μa	Melt composition, wt. % Na_2WO_4	WO_3
cathodic	1105	ca. 560	100	0
cathodic	1106	1160	89.8	10.2
cathodic	1106	1240	80.0	20.0
cathodic	1106	1100	60.0	40.0
anodic	1105	660	100	0
anodic	1106	1285	89.8	10.2
anodic	1106	1290	80.0	20.0
anodic	1106	1130	60.0	40.0

data to concentration polarization. Anodic polarization was studied by Flood and Förland (62), Karpatscheff and Patzug (73), and Janz and Colom (59). These workers all explained their data in terms of activation overpotential.

The Tafel equation

$$\eta_A = a + b \log I$$

can be rewritten in the form

$$\eta_A = \frac{RT}{\alpha nF} \ln \frac{I}{I_o}$$

where I_o is a constant, α is a symmetry coefficient (often on the order of 0.5), and the other symbols have their usual significance (8). Janz and Colom (59) and Flood and Förland (62) let $\alpha = 0.5$ and $n = 2$. Their equation then was reduced to the form

$$\eta_A = \frac{RT}{F} \ln \frac{I}{I_o} .$$

Note that the anodic concentration overpotential equation

assumed in the present research takes on the same form at sufficiently large values of cell current, i.e.,

$$\eta_C \cong \frac{RT}{F} \ln \frac{I}{I_\ell} .$$

The data obtained on graphite electrode polarization were much more difficult to interpret than were the corresponding platinum results. There were several reasons for this. Perhaps the most serious difficulty arose from the non-reproducibility of results from day to day, or even hour to hour. The graphite data were considerably more variable than were the platinum data. This variability was all the more troublesome in view of the generally smaller magnitudes of overpotential of graphite than of platinum.

At any given cell current, graphite overpotentials were quite slow in reaching stable values. The rate of attainment of stability was not strongly temperature dependent; however, short term voltage fluctuations became serious at temperatures in excess of about 900°. These fluctuations introduced further uncertainty in the data. Overpotentials were recorded three minutes after setting each new cell current value. When current either was increased from a prior value or simply switched on, η reached about 90% of its ultimate value for that particular current in three minutes. Similar behavior was noted when current was reduced or switched off.

Representative graphite polarization curves are shown

in Figure 14. It is evident from inspection of these curves that, at least in the cell current range illustrated, the overvoltages do not suddenly increase without limit. Such behavior would be demanded by the concentration overpotential equation which is derived for the case of a potential-determining ion diffusing in toward the electrode.

A series of runs was made at various temperatures in which very high cell currents were employed. No apparent breaks or discontinuities in the anodic curves were observed at cell currents up to 310 milliamperes. Some of the cathodic curves displayed breaks at cell currents on the order of 5 milliamperes. Tungsten bronze crystals were formed on graphite cathodes under high current conditions. Even at cell currents up to 310 ma (anodic polarization) the Tafel equation was not obeyed.

Data were analyzed in much the same fashion as were the platinum polarization results. Values of n were chosen such that a plot of exponential ($nF\eta/RT$) vs. I gave a straight line. The anodic overpotential data for graphite obeyed the equation

$$\eta = \frac{RT}{F} \ln \left(1 + \frac{I}{I_\ell}\right).$$

The cathodic polarization results also fit the same equation, providing absolute values of η were used. That is, unlike for the platinum data, negative overvoltages did not lead to linear plots. Such behavior can be justified by the

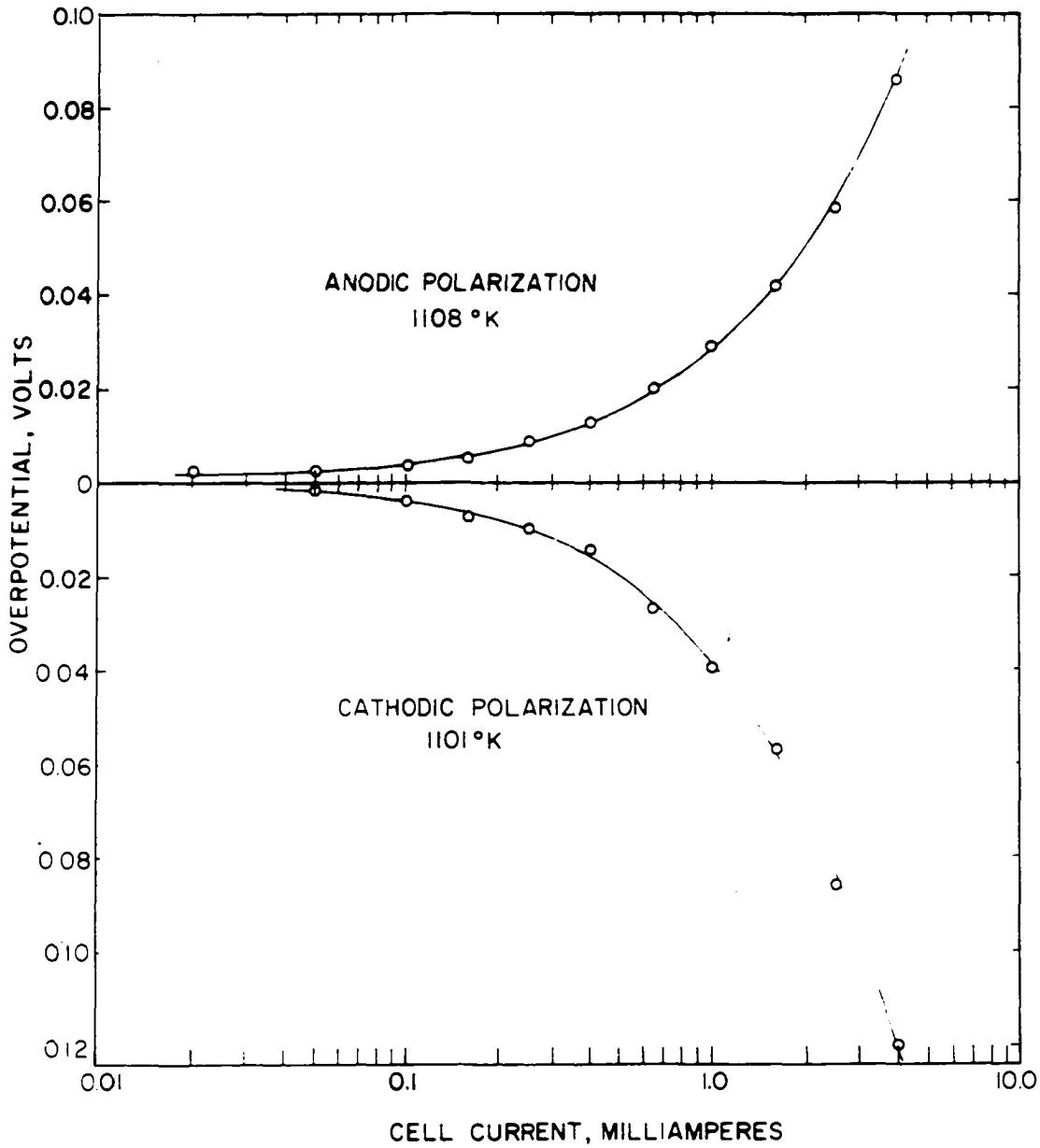

Figure 14. Polarization of carbon, carbon dioxide electrodes

assumption that outward diffusing species were responsible for both anodic and cathodic polarization.

Two typical sets of polarization data are presented in Figure 15 in a manner designed to illustrate the closeness of agreement of experimental points with the calculated equations. Table 8 compares the anodic and cathodic limiting currents at two temperatures. The temperature dependence of anodic limiting current is indicated in Table 9. The effect of melt composition on graphite limiting current was studied briefly. The results are given in Table 10.

The rate of decay of anodic overpotential of graphite was followed with an X-Y recorder. Rates were measured at various temperatures and cell currents, and found to be neither linear nor logarithmic with respect to time.

Table 8. Graphite polarization limiting currents

Type of polarization	Temperature, °K	I_ℓ, μa
anodic	1041	785; 1440[a]
anodic	1108	2900
cathodic	1041	525
cathodic	1101	2050

[a]At lower temperatures, a sharp break always was observed in plots of exponential ($nF\eta/RT$) *vs*. I for the anodic data. The curve on either side of the break always was linear.

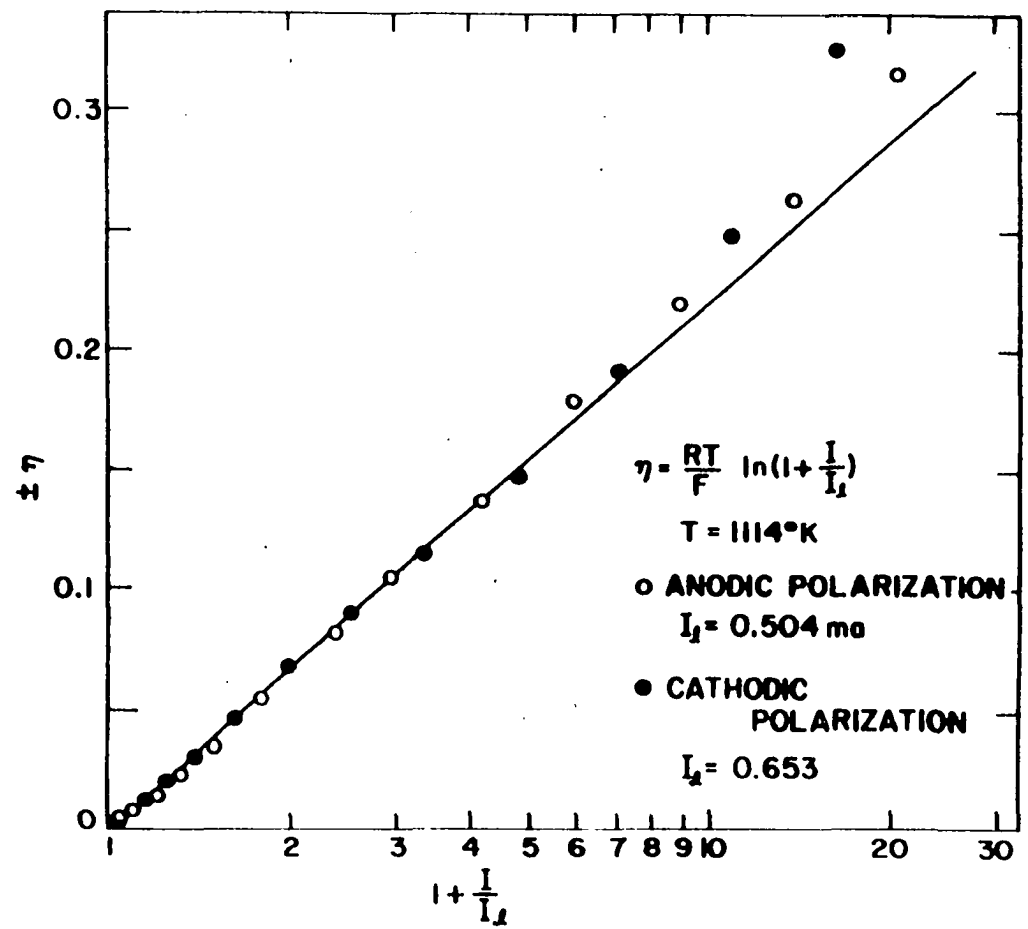

Figure 15. Illustration of the correspondence of graphite polarization data to calculated equations

Table 9. Temperature dependence of graphite anodic limiting current

Temperature, °K	I_ℓ,[a] μa
975	330; 575[b]
1048	665; 1065[b]
1113	2065
1175	4125

[a] $\frac{d \ln I_\ell}{dt} = .0105 \text{ deg}^{-1}$.

[b] See footnote in Table 8.

Table 10. Dependence of graphite electrode limiting current on melt composition

Type of polarization	Temperature, °K	I_ℓ, μa	Melt composition, wt. % Na_2WO_4	WO_3
anodic	1110	750	100	0
anodic	1110	1592	89.2	10.2
anodic	1110	1800	80.2	19.8
anodic	1110	2586	60.0	40.0
cathodic	1110	765	100	0
cathodic	1110	820	89.2	10.2
cathodic	1110	1074	80.2	19.8
cathodic	1110	2757	60.0	40.0

Published information on graphite anodic polarization in oxy-anionic melts is extremely limited. With the exception of one study with the melt KCl-NaCl-Na_2SO_4 (79), all investigations have been made with cryolite-Al_2O_3 melts. In such melts the overpotential-current relationship is complex and

apparently consists of three distinct regions as current density is increased from zero to 0.3 amp cm^{-2} (80,81,82). At low currents ($\leq$0.1 amp cm^{-2}) Karpachev, Rempel', and Iordan (83) reported overpotential to follow the Tafel equation. The workers cited above and others (50,84,85) also have reported that the final overpotential reached at any given cell current was attained slowly. The low current results generally have been interpreted as arising from the formation of surface oxides of graphite. Once the surface oxides are formed, bond rearrangements occur and eventually CO_2 and CO are desorbed. The slowness of bond reformation and gas evolution are proposed to be the cause of anodic overpotential.

The nature of the oxygen-containing ions in cryolite-alumina melts is uncertain. It does not follow necessarily that graphite anodes would behave in other oxy-melts in the same fashion as they do in alumina systems, although Rempel' (79) did invoke a carbon sub-oxide mechanism to explain his KCl-NaCl-Na_2SO_4 results. As has been stated previously, the concentration overpotential equations assumed in the present research was of the same form as the Tafel overpotential equation. The latter equation would be obeyed if some activated process (such as formation and desorption of CO_2 or CO) were to be postulated.

Further study of graphite anodic polarization in a vari-

ety of oxy-anionic melts is warranted. These investigations become especially pertinent for work directed toward the development of useful carbon fuel cells.

SUMMARY

An electrochemical cell was developed wherein graphite and oxygen were consumed and carbon dioxide and carbon monoxide were formed at the electrodes. The cell consisted of a reversible platinum, oxygen cathode, a graphite anode, and an oxy-anionic electrolyte of fused Na_2WO_4-WO_3 mixture.

Very nearly the thermodynamically calculable cell voltages were observed in preliminary experiments involving $Na_2B_4O_7$-B_2O_3 melts. Voltages in tungstate melts were approximately 20% lower. It was postulated that the low results arose from reduction or dissociation of the melt. Two mechanisms were suggested which would predict low voltages. One mechanism invoked tungsten bronze formation at the graphite-melt interface and the creation thereby of a secondary cell. The other mechanism assumed the existence of an oxygen concentration cell with the graphite electrode oxygen pressure governed by dissociation of the melt.

Anodic and cathodic overvoltages developed at each electrode were studied. The platinum, oxygen electrode was found to exhibit concentration overpotential when it functioned either as an anode or as a cathode. Behavior of the graphite electrode was difficult to interpret. The data satisfied equations for concentration overpotential if it was assumed that the electrochemically active species involved for both anodic and cathodic processes were diffusing away

from the electrode. Other workers have proposed that anodic polarization arises from an activated process involving the formation of surface oxides of carbon. The data obtained in the present research did not permit a choice between the two proposed mechanisms.

In all four cases of electrode polarization which were studied, the number of electrons transferred in the rate-determining step was one.

ACKNOWLEDGMENTS

The encouragement offered and the scientific and personal philosophy expressed by Professor Frederick R. Duke are deeply appreciated. The author is especially grateful for the patient understanding shown and the many sacrifices made by his wife, Mary, during the course of this work.

The author is grateful to the Department of the Air Force for the financial support which made possible his attendance at Iowa State University.

LITERATURE CITED

1. Andrews, L. V. and W. E. Martin, J. Am. Chem. Soc., 60, 871 (1938).

2. Newberry, E., J. Chem. Soc., 113, 701 (1919).

3. Gunning, H. E. and A. R. Gordon, J. Chem. Phys., 10, 126 (1942).

4. Kell, G. S. and A. R. Gordon, J. Am. Chem. Soc., 81, 3207 (1959).

5. Ives, D. J. G. and S. Swaroopa, Trans. Faraday Soc., 49, 788 (1953).

6. Brönsted, J. N. and R. F. Nielsen, Trans. Faraday Soc., 31, 1478 (1935).

7. Eastman, E. D., J. Am. Chem. Soc., 42, 1648 (1920).

8. Glasstone, Samuel. An introduction to electrochemistry. New York, N. Y., D. Van Nostrand Company, Inc. 1942.

9. Poincaré, M. L., Ann. Chim. (Paris), Ser. 6, 21, 289 (1890).

10. Grantham, L. F. and S. J. Yosim, [The electrical conductivities of molten bismuth-bismuth triiodide solutions, J. Chem. Phys., to be published ca. 1963].

11. Bloom, H., I. W. Knaggs, J. J. Molloy and D. Welch, Trans. Faraday Soc., 49, 1458 (1953).

12. Doucet, Y. and M. Bizouard, Bull. Soc. Chim. France, 1959, 1570.

13. Doucet, Yves and Michel Bizouard, Compt. Rend., 248, 1328 (1959).

14. Goodwin, H. M. and R. D. Mailey, Phys. Rev., 26, 28 (1908).

15. Jaeger, F. M. and B. Kapma, Z. Anorg. Allgem. Chem., 113, 27 (1920).

16. Kröger, Carl and Peter Weisgerber, Z. Physik. Chem. (Frankfurt), 5, 192 (1955).

17. Markov, B. F. and A. M. Tarasenko, Zh. Fiz. Khim., 32, 1333 (1958).

18. Murgulescu, I. G. and S. Zuca, Acad. Rep. Populare Romini, Studii Cercetari Chim., 7, 325 (1959).

19. Polyakov, V. D., Izv. Sektora Fiz. Khim. Analiza, Inst. Obshch. Neorgan. Khim., Akad. Nauk SSSR, 26, 147 (1955).

20. Popovskaya, N. P. and P. I. Protsenko, Zh. Neorgan. Khim., 7, 2237 (1962).

21. Protsenko, P. I. and N. P. Popovskaya, J. Gen. Chem. USSR (English Transl.), 24, 2089 (1954).

22. Sandonnini, C., Gazz. Chim. Ital., 50, Part 1, 289 (1920).

23. Jones, G. and B. C. Bradshaw, J. Am. Chem. Soc., 55, 1780 (1933).

24. Hodgman, Charles D., Robert C. Weast and Samuel M. Selby, eds. Handbook of chemistry and physics. 42nd ed. Cleveland, Ohio, Chemical Rubber Publishing Co. 1960.

25. Inman, D., J. Sci. Instr., 39, 391 (1962).

26. Diehl, Harvey and G. Frederick Smith. Quantitative analysis. New York, N. Y., John Wiley and Sons, Inc. 1952.

27. Duke, F. R. and H. M. Garfinkel, J. Phys. Chem., 65, 461 (1961).

28. Owen, Benton Brooks and Frederick Humphrey Sweeton, J. Am. Chem. Soc., 63, 2811 (1941).

29. Stokes, R. H., J. Phys. Chem., 65, 1242 (1961).

30. Worthing, Archie G. and Joseph Geffner. Treatment of experimental data. New York, N. Y., John Wiley and Sons, Inc. 1943.

31. Smith, G. Pedro and Guy F. Petersen, J. Chem. Eng. Data, 6, 493 (1961).

32. Murgulescu, I. G. and C. Volanschi, Rev. Chim., Acad. Rep. Populaire Roumaine, 6, 45 (1961).

33. Karpachev, S. V., A. G. Stromberg and V. N. Podchainova, Zh. Obshch. Khim., 5, 1517 (1935).

34. Van Artsdalen, E. R. and I. S. Jaffe, J. Phys. Chem., 59, 118 (1955).

35. Duke, Frederick R. and George Victor, J. Am. Chem. Soc., 83, 3337 (1961).

36. Laity, Richard W. and Corneluis T. Moynihan, J. Phys. Chem., 67, 723 (1963).

37. Young, G. J. and R. B. Rozelle, J. Chem. Educ., 36, 68 (1959).

38. Liebhafsky, H. A. and D. L. Douglas. Introduction. In Young, G. J., ed. Fuel cells. pp. 1-10. New York, N. Y., Reinhold Publishing Corp. 1960.

39. Baur, Emil and H. Ehrenberg, Z. Elektrochem., 18, 1002 (1912).

40. _____, Agnes Petersen and G. Füllemann, Z. Elektrochem., 22, 409 (1916).

41. _____, W. D. Treadwell and G. Trümpler, Z. Elektrochem., 27, 199 (1921).

42. _____ and Roland Brunner, Z. Elektrochem., 41, 794 (1935).

43. _____ and _____, Z. Elektrochem., 43, 725 (1937).

44. _____ and Hans Preis, Z. Elektrochem., 43, 727 (1937).

45. _____, Brennstoff-Chem., 20, 385 (1939).

46. _____ and Jakob Tobler, Z. Elektrochem., 39, 169 (1933).

47. Murgulescu, I. G. and S. Sternberg, Discussions Faraday Soc., 32, 107 (1961).

48. Rose, B. A., G. J. Davis and H. J. T. Ellingham, Discussions Faraday Soc., 4, 154 (1948).

49. Treadwell, W. D., Z. Elektrochem., 22, 414 (1916).

50. Mashovets, V. P. and A. A. Revazyan, J. Appl. Chem. USSR (English Transl.) 30, 1069 (1957).

51. Hill, Douglas G., Bernard Porter and Arthur S. Gillespie, Jr., J. Electrochem. Soc., 105, 408 (1958).

52. Delimarskii, Yu. K. and V. N. Andreeva, Dopovidi Akad. Nauk Ukr. RSR, 1959, 760.

53. _____ and _____, Russ. J. Inorg. Chem. (English Transl.) 5, 873 (1960).

54. _____ and G. D. Nazarenko, Ukr. Khim. Zh., 27, 458 (1961).

55. Washburn, Edward W., ed. International critical tables. Vol. 4. New York, N. Y., McGraw-Hill Book Co., Inc. 1928.

56. Duke, F. R. and James L. Copeland, [Graphite-oxygen high-temperature fuel cell, J. Electrochem. Soc., to be published ca. 1963].

57. Ives, D. J. G. Oxide, oxygen, and sulfide electrodes. In Ives, David J. G. and George J. Janz, eds. Reference electrodes; theory and practice. pp. 322-392. New York, N. Y., Academic Press. 1961.

58. Janz, G. J. and F. Saegusa, Electrochim. Acta, 7, 393 (1962). Original not available; abstracted in Chemical Abstracts 57, 7013d (1962).

59. _____ and Francisco Colom. U. S. Atomic Energy Commission Report ONR-148566 [Office of Naval Research, Washington, D. C.]. 1959.

60. Stepanov, G. K. and A. M. Trunov, Dokl. Akad. Nauk SSSR, 142, 866 (1962).

61. Flood, H., T. Förland and K. Motzfeldt, Acta Chem. Scand., 6, 257 (1952).

62. _____ and _____, Discussions Faraday Soc., 1, 302 (1947).

63. Lux, Hermann, Z. Elektrochem., 45, 303 (1939).

64. Csaki, Paul and Adolf Dietzel, Glastech. Ber., 18, 33 (1940).

65. Delimarskii, Yu. K., V. N. Andreeva and G. D. Nazarenko. Thermodynamic properties of oxides dissolved in molten sodium metaphosphate and in borax. In Transactions of the All-Union Conference on Physical Chemistry of Molten Salts and Slags, Sverdlovsk, Nov. 22-25, 1960. pp. 442-453. Moscow, USSR, Metallurgizdat. 1962. Original not available; abstracted in Chemical Abstracts, 57, 15889e (1962).

66. Nazarenko, G. D., Ukr. Khim. Zh., 27, 618 (1961). Original not available; abstracted in Chemical Abstracts, 56, 8462d (1962).

67. Delimarskii, Yu. K. and V. N. Andreeva, Dopovidi Akad. Nauk Ukr. RSR, 1959, 633.

68. Didtschenko, Rostislav and Eugene G. Rochow, J. Am. Chem. Soc., 76, 3291 (1954).

69. Agar, J. N. and F. P. Bowden, Proc. Roy. Soc. (London), Ser. A, 169, 220 (1939).

70. Kust, Roger Nayland. A study of the nitrate ion dissociation in fused nitrates. Unpublished Ph.D. thesis. Ames, Iowa, Library, Iowa State University of Science and Technology. 1963.

71. Shams El Din, A. M., Electrochim. Acta, 7, 285 (1962). Original not available; abstracted in Chemical Abstracts, 57, 6691b (1962).

72. _____ and A. A. A. Gerges, J. Electroanal. Chem., 4, 309 (1962).

73. Karpatscheff, S. and W. Patzug, Z. Physik. Chem. (Leipzig), 173, 383 (1935).

74. Delimarskii, Iu. K. and B. F. Markov. Electrochemistry of fused salts. Translated by Adam Peiperl. Washington, D. C., The Sigma Press, Publishers. 1961.

75. Lewis, Gilbert Newton and Merle Randall. Thermodynamics. 2nd ed. New York, N. Y., McGraw-Hill Book Co., Inc. 1961.

76. Datta, A. K. and N. Dhar, J. Am. Chem. Soc., 38, 1156 (1916).

77. Kortüm, G. and J. O'M. Bockris. Textbook of electrochemistry. Vol. 2. New York, N. Y., Elsevier Publishing Co. 1951.

78. Agar, J. N. and F. P. Bowden, Proc. Roy. Soc. (London), Ser. A, 169, 206 (1939).

79. Rempel', S. I., Dokl. Akad. Nauk SSSR, 117, 648 (1957).

80. Antipin, L. N. and A. N. Khudyakov, Dokl. Akad. Nauk SSSR, 100, 93 (1955).

81. _____ and _____, Zh. Prikl. Khim., 29, 908 (1956).

82. _____ and V. K. Dudyrev, Zh. Fiz. Khim., 31, 2032 (1957).

83. Karpachev, S., S. Rempel' and E. Iordan, Zh. Fiz. Khim., 23, 422 (1949).

84. Rempel', S. I. and L. P. Khodak, Dokl. Akad. Nauk SSSR, 75, 833 (1950).

85. _____ and _____, Zh. Prikl. Khim., 26, 931 (1953).